Prairie Vole Model Organism Development and Validation

by
Gina Williams

DISSERTATION
Submitted in partial satisfaction of the requirements for degree of
DOCTOR OF PHILOSOPHY

in

Neuroscience

in the

GRADUATE DIVISION
of the
UNIVERSITY OF CALIFORNIA, SAN FRANCISCO

Approved:

DocuSigned by:
Vikaas Sohal
70A483C8DEB04E6...

Vikaas Sohal
Chair

DocuSigned by:
DEVANAND MANOLI

DocuSigned by:
Dena Dubal

Dena Dubal

DocuSigned by:
Helen Willsey
CAA5EAC85A9B44D...

Helen Willsey

Committee Members

Acknowledgments

I would like to thank everyone in the Manoli Lab and Bender Lab who contributed to these projects. Particularly, Nerissa Hoglen and Josh Steigner, and Nanditha Krishnan and Sunrae Taloma in the Bender Lab for their hard work on the *Scn2a*$^{-/+}$ characterization project. Additionally, I would like to acknowledge Ruchira Sharma and Mike Sherman for being part of the transgenesis team.

Prairie Vole Model Organism Development and Validation

Gina Williams

Abstract

Interrogating the neurobiology underlying ASD pathology in traditional animal models is hampered by limited social behaviors in these species. Prairie voles display diverse, robust social behaviors and long-term relationships. Comparative studies suggest that the neural and genetic mechanisms mediating such attachments and complex social behaviors may be conserved across mammals. These prairie voles are therefore a powerful system to understand the biology of neuropsychiatric conditions characterized by the disruption of social behaviors, such as autism spectrum disorder (ASD). To capitalize on this model, we generated prairie voles bearing loss of functional alleles of *Scn2a*, a high-confidence ASD-associated gene, and characterized the social behaviors of adult heterozygous mutants. *Scn2a* encodes for the neuronal sodium channel $Na_V1.2$ whose function has been studied well in mouse models. We find here that heterozygous loss of Scn2a in voles results in comparable changes in $Na_V1.2$-dependent aspects of neuronal excitability. We assessed the social dynamics of heterozygous male and female Scn2a mutant prairie voles as compared to wildtype siblings through a battery of behavioral assays to determine how heterozygosity for *Scn2a* impacted social and attachment behaviors at multiple timepoints throughout pair bonding. We further investigated vocal dynamics of *Scn2a*$^{-/+}$ males and females during the initial interactions with novel opposite sex animals. We found that mutants *heterozygous* for *Scn2a* display distinct, *sex-specific,* and context-specific differences in social dynamics across bonding. *Scn2a*$^{-/+}$ adult male prairie voles display atypical affiliative behavior with a novel stranger as compared to wildtype siblings, regardless of bonding status. These experiments lay the groundwork to uncover potential biological mechanisms underlying social deficits in genetic models of ASD and determine if the neural or genetic differences observed in mutants persist throughout the lifespan.

TABLE OF CONTENTS

LIST OF FIGURES

LIST OF TABLES

Chapter 1: Scn2a$^{-/+}$ prairie vole behavior

Introduction

Attachment between individuals lies at the core of human relationships at all levels of social interaction. The formation and maintenance of relationships necessary for the survival of a species are driven by innate social behaviors. In rare cases, such as humans and prairie voles, these behaviors include the formation of enduring attachments between peers and mates[1–3]. Autism spectrum disorder (ASD) is a highly prevalent neurodevelopmental disorder that profoundly impacts individuals' social interactions and attachments[4]. Differences in social behavior present early in life and persist throughout adulthood. However, the symptoms experienced by individuals with ASD can vary greatly from person to person. Furthermore, while many genes have been identified as high-risk when mutations are present in humans, how these and other risk factors alter development to give rise to the symptoms of ASD are poorly understood.

Human genetic studies have identified *SCN2A* as a high-risk ASD gene and suggest that haploinsufficiency from heterozygous loss of function (LOF) mutations contributes to the development of the disorder, though the underlying pathology is unknown[5–8]. Some behavioral studies of mouse models of *Scn2a* haploinsufficiency have found juvenile and adult phenotypes[9–11]. However, as most studies of *Scn2a* investigate physiology, determining behavioral phenotypes and the disruptions to the neural circuits that underlie these behaviors throughout the life of the animal is needed[9].

Model organisms made to bear mutations in such genes are often used to better understand their impacts on the development of the nervous system and behavior. However, interrogating the neurobiology underlying symptoms of ASD in traditional animal models is hampered by limited social and attachment behaviors in the species most commonly used as such models. Therefore, there is very little evidence of effects of heterozygous mutations in these organisms[12–14]. Prairie voles display sexually dimorphic social attachment in the formation of pair

bonds between mates and peer affiliation between peers [1–3,15]. This species provides a powerful and unique advantage when studying psychiatric disorders characterized by social deficits, like ASD, because of these distinct and robust social behaviors, allowing us to unmask more subtle effects of ASD-like mutations.

We therefore developed molecular genetic approaches in highly social prairie voles, which display diverse, robust social behaviors and long-term relationships across the lifespan. Specifically, we generated prairie vole lines bearing LOF alleles of *Scn2a* and validated the functional loss of these mutations using slice electrophysiology in the prefrontal cortex (PFC). We then assayed differences in pair bonding and maintenance behavior, as well as general social behavior patterns, by using our previously established battery of pair bonding assays. Using these approaches, we uncovered a male-specific difference in social behavior of Scn2a heterozygous mutants compared to wildtype siblings, such that adult *Scn2a*$^{-/+}$ males are more affiliative with adult wildtype female stims regardless of bonding-status and female identity. All together, we have shown the prairie vole to be a powerful and sensitive system for studying social behavior and neuropsychiatric disorder models and have uncovered specific social behavioral differences in one of these models that lays the foundation for uncovering underlying neural differences that contribute to these behavioral differences.

Results

Generation and validation of mutants (Electroporation/CRISPR)

Given the unique social behaviors of the prairie vole, we wanted to establish the system as a robust model organism for studying the impacts of genetic mutations associated with social disorders, including ASD. To achieve this, we first developed a protocol that utilizes the CRISPR/Cas9 system and electroporation of single-cell embryos (Fig. 1A) for mutagenesis. This is a modified version of our previous approach of making mutant voles that used microinjections[16]. We electroporated Cas9 mRNA, Cas9 protein, and short guide RNAs (sgRNA) with sequences

matching the prairie vole Scn2a locus (Fig. 1B). The embryos were cultured in vitro to the blastocyst stage, then implanted into a pseudopregnant female. The pups born from the implanted female were considered the G0 generation and screened for mutations at the Scn2a locus using PCR and Sanger Sequencing. We generated 3 alleles in the Scn2a locus: an in-frame 108 base pair deletion in exon 1 (Exon 1a), an in-frame 12 base pair deletion in exon 1 (Exon 1b), and a protein-truncating 2 base pair deletion in exon 3 (Exon 3) (Fig. 1C). We moved forward with 2 of these mutations - the Exon1a deletion and the Exon3 deletion. Given the potential for off-target mutations from the CRISPR manipulation, we then outbred these alleles, alternating the sex of the affected animal in a pair, for seven generations[17]. Once we reached the F7 generation, we proceeded with validating the mutations and characterizing the behavior.

Electrophysiology validation of loss of function of Exon 1a and Exon 3 deletions

To confirm that the Exon 1a and Exon 3 mutations resulted in loss of function of Nav1.2, we used current-clamp slice electrophysiology in pyramidal neurons in the prefrontal cortex (PFC) (Fig. 2A). We performed the same experiments in male and female voles of each genotype (*Scn2a*$^{-/+}$ and WT siblings), aged ~P30, roughly the age at which the expression and function of NaV1.2 has stabilized in WT mice.

As expected from similar mouse studies, we found that the action potential (AP) peak dV/dt was significantly lower in *Scn2a*$^{\Delta 1a/+}$ and *Scn2a*$^{\Delta 3/+}$ animals, a metric reflecting the decreased density of functional $Na_V1.2$ channels on the neuronal soma (Fig. 2B). We also found that there is a decreased AP amplitude in the *Scn2a* heterozygous animals, reflecting shorter spikes and less depolarization and therefore recruiting fewer voltage-gated potassium channels (Fig. 2C). While this does not affect the after hyperpolarization (AHP) in *Scn2aΔ1a/+* voles, it does result in a significantly lower AHP in *Scn2aΔ3/+* voles, which could be due to the differences in the nature of the mutations (Fig. 2D).

Unexpectedly, the AP threshold was significantly lower in *Scn2a*$^{\Delta 1a/+}$ and *Scn2a*$^{\Delta 3/+}$ voles compared to WT siblings (Fig. 2E) despite there being no difference in resting membrane potential or input resistance in either genotype (Fig. 2F,G). Consequently, the number of APs in each genotype increases with increasing currents, a "bursty" phenotype (Fig. 2H). Though this physiological phenotype has not been previously shown in other rodent models of *Scn2a* haploinsufficiency, the main findings of decreased peak dv/dt and decreased AP amplitude are consistent with other models.

These results confirm that each of the mutations have resulted in a loss of function of NaV1.2 in our prairie vole models. There were no observable sex differences, and each genotype showed extremely similar phenotypes despite being generated from different alleles. Given that the alleles both are loss of function mutations, we chose to perform the behavioral characterization experiments in *Scn2a*$^{\Delta 1a/+}$.

$Na_V1.2$ haploinsufficiency does not impact partner preference after cohabitation

In order to understand the impacts of *Scn2a* heterozygosity on typical prairie vole attachment, we ran adult *Scn2a*$^{\Delta 1/+}$ males and females through a version of our adult attachment behavior battery of assays[8]. Adult *Scn2a*$^{\Delta 1/+}$ females and WT siblings were first tested on a truncated sensitized timeline of just an introduction and a partner preference test (PPT). In these PPTs, we secure the cohabitated male partner of an *Scn2a*$^{\Delta 1a/+}$ female or WT sibling on one side of a three-chamber lane and a male stranger on the other side, allowing the female to move freely between the chambers (Fig. 3A). These PPT assays begin exactly 6 hours after the Introduction assay (Fig. 3B). We started with this sensitized timeline because previous experiments in the lab have shown that WT females and WT female siblings of other genetic models are able to show robust partner preference after just 6 hours of cohabitation[16]. However, we found that in our cohort, there was no significant difference in time spent in the partner chamber or stranger chamber in either WT or *Scn2a*$^{\Delta 1a/+}$ females, and no significant difference in time spent huddling

with the partner or the stranger (Fig. 3C,D). When we reduce huddle time with partner and stranger to a Partner Preference Index (PPI), we again find no difference between *Scn2a*$^{\Delta 1a/+}$ females and female WT siblings, and a wider spread of PPIs in the WT cohort (Fig. 3E).

To ensure more robust female partner preference, we used a timeline with a longer period of cohabitation for females (24 hours post-Timed Mating assay, or 72 hours post-Introduction assay) for our longitudinal battery of assays (Fig. 3F). At this time point, we now find that both *Scn2a*$^{\Delta 1a/+}$ females and female WT siblings show an increased time spent in the partner chamber and increased time huddling with partners as compared to strangers (Fig. 3G,H). We consequently did not find any significant group differences in PPI between Scn2a$^{\Delta 1a/+}$ female voles and their female WT siblings after sufficient cohabitation (Fig. 3I).

We similarly performed the PPT in *Scn2a*$^{\Delta 1a/+}$ males and male WT siblings as part of a longitudinal battery of assays, though the timeline differs such that these PPTs occur 72 hours post-Timed Mating assay, or 120 hours post-Introduction[8]. We found a significant increase in time spent in the female partner chamber compared to a stranger female in WT sibling males, but this difference was not found in *Scn2a*$^{\Delta 1a/+}$ males (Fig. 3J). However, we did find that both *Scn2a*$^{\Delta 1a/+}$ males and male WT siblings spent significantly more time with their female partners compared to stranger females (Fig. 3K). This is again reflected in the lack of significant difference in PPI between *Scn2a*$^{\Delta 1a/+}$ males and WT siblings (Fig. 3L). These data suggest that $Na_V1.2$ haploinsufficiency does not impact male or female prairie voles' ability to form a pair bond with a cohabitated partner.

$Na_V1.2$ haploinsufficiency leads to increased affiliative behavior in male prairie voles during initial interactions

Though partner preference is intact in our *Scn2a*$^{\Delta 1a/+}$ animals, we still wanted to assess the impact of $Na_V1.2$ haploinsufficiency on other aspects of social behavior related to the pair bonding process. We started each battery by recording the behaviors of naive *Scn2a*$^{\Delta 1a/+}$ animals

and their WT siblings when first introduced to the naive opposite-sex, age-matched WT vole that they will cohabitate with for the duration of the timeline ("Introduction", Fig. 4A). We manually scored these behaviors and broke them down into 2 categories: affiliative behaviors (non-anogenital sniffing, anogenital sniffing, and side-by-side huddling) and agonistic behaviors (striking, tussling).

We found no differences in any behaviors when comparing female *Scn2a*$^{\Delta 1a/+}$ to WT siblings in this context. Male *Scn2a*$^{\Delta 1/+}$ animals, however, showed a significant difference in total time spent engaged in affiliative behavior with the novel female (Fig. 4B). This could potentially be due to a difference in behavior in the female animal, but we did not see any differences in the frequency of strikes by the WT female toward the *Scn2a*$^{\Delta 1a/+}$ males compared to male WT siblings (Fig. 4C). We also did not see any difference in agonistic behaviors directed toward the WT female in *Scn2a*$^{\Delta 1a/+}$ males compared to male WT siblings (Fig. 4D).

We next looked at the individual behaviors that contribute to the increased time spent in affiliative behavior. We first observed that WT sibling males and *Scn2a*$^{\Delta 1a/+}$ males displayed different proportions of specific affiliative behaviors (Fig. 4E). When we assess different aspects of each of the affiliative behaviors, we find that *Scn2a*$^{\Delta 1a/+}$ males display more instances of non-anogenital sniffs compared to WT siblings, but not longer bouts of non-anogenital sniffs or total time (Fig. 4F). Therefore, non-anogenital sniffs are not contributing to the increase of total time engaged in affiliative behavior.

Scn2a$^{\Delta 1a/+}$ males also spend more overall time anogenital-sniffing the novel female (Fig. 4G). This is seemingly driven by an increase in mean duration of anogenital sniff bouts, as the frequency of anogenital sniffing is not different between groups (Fig. 4H-I). Total time spent engaged in side-by-side huddling was also increased in *Scn2a*$^{\Delta 1a/+}$ males compared to WT siblings (Fig. 4J). This increase is driven by both a significant increase in the number of bouts of huddling as well as a significant increase in bout mean duration (Fig. 4K-L). Therefore, *Scn2a*$^{\Delta 1a/+}$ males engage in longer sniffs and longer huddles with naive WT females, as well as more huddles

with this female, despite the WT female not displaying less agonistic behavior toward the *Scn2a*$^{\Delta 1a/+}$ males.

These results suggest *Scn2a* haploinsufficiency in the prairie vole disrupts the regulation of context-appropriate affiliative behavior in a sex-specific manner such that *Scn2a*$^{\Delta 1/+}$ males will engage in all affiliative behaviors with a stranger female more than male WT siblings. While these males are hyperactive in that they have more total events scored over the course of the assay, they do not display hyperactive behavior in the open field test (OFT) (Fig. 9G,J). Therefore, this hyperactivity is influenced by the presence of the naive WT female and thus social-context specific rather than a general phenotype.

$Na_V1.2$ haploinsufficiency induces exploration and affiliation with a stranger female, but does not decrease aggression, in pair-bonded male prairie voles

In order to test the effects of $Na_V1.2$ haploinsufficiency on social behavior after the formation of a pair-bond, we used our Partner Reunification and Stranger Rejection assays (Fig. 5A). Briefly, these assays are used to survey the behavior of our subject animal after a stressful period (being removed from partner) and then put into one of two contexts, reunification with the partner or exposure to a novel, naive opposite-sex stimulus animal (Fig. 5B). Similar to the Introduction assay, we did not find any significant differences in female *Scn2a*$^{\Delta 1/+}$ behavior, affiliative or agonistic, compared to WT siblings in either the Partner Reunification or Stranger Rejection assays.

In the Stranger Rejection assay, however, we found that *Scn2a*$^{\Delta 1a/+}$ males show significant differences in their affiliative behavior toward the novel, naive female, despite showing intact partner preference (Fig. 5C). Specifically, we found that Scn2a$^{\Delta 1a/+}$ males spent more total time engaged in side-by-side huddling, potentially driven by the significant difference in frequency of huddles as the mean huddle duration does not differ between *Scn2a*$^{\Delta 1a/+}$ males and WT sibling males (Fig. 5D-E). However, *Scn2a*$^{\Delta 1a/+}$ males display comparable counts of agonistic behaviors

towards the stranger female as compared to WT siblings, providing further evidence that the observed difference in affiliative behavior is not due to a pair bonding deficit (Fig. 5F).

Given that side-by-side-huddling is a highly affiliative behavior and unexpected in the context of the Stranger Rejection assay, we wanted to assess if there are differences in the likelihood of affiliative behaviors occurring. We made a Markov Chain transition matrix for the behaviors exhibited by *Scn2a*$^{\Delta 1a/+}$ males and WT sibling males in the Stranger Rejection assay and found that *Scn2a*$^{\Delta 1a/+}$ males were significantly more likely to transition into a huddle after an anogenital sniff (63/712 or 9% in *Scn2a*$^{\Delta 1a/+}$ males vs. 9/363 or 2% in WT sibling males, p-value = 0.00013; Fig. 5G). While the absolute number of anogenital sniffs by *Scn2a*$^{\Delta 1a/+}$ males is nearly double that of WT sibling males, the population distribution is not significantly different (Fig. 5H). The anogenital sniff duration distributions also do not significantly differ between *Scn2a*$^{\Delta 1a/+}$ males and their WT siblings (Fig. 5I). However, we do see a difference in the distribution of anogenital sniff durations preceding a side-by-side huddle such that *Scn2a*$^{\Delta 1a/+}$ males are more likely to transition into a side-by-side huddle after shorter anogenital sniffs compared to WT sibling males (Fig. 5J).

Overall, these data suggest a sex-specific impact of $Na_V1.2$ haploinsufficiency on appropriate stranger-directed behavior such that *Scn2a*$^{\Delta 1/+}$ males display atypical patterns of affiliative behavior toward stranger females, despite intact partner preference and no change in stranger-directed agonistic behavior. These data reinforce the concept that attachment behavior in prairie voles is modular and therefore aspects of pair-bonding may be impacted differently with the same genetic manipulation.

Naive male or female Scn2a$^{\Delta 1a/+}$ *voles are approached differently than WT siblings by novel WT animals*

If the opposite-sex WT freely moving animals as a population skew toward a preference of one genotype over the other, it could have implications for the attachment behavior results and

interpretation of phenotypes. In order to test whether there is an inherent attractive or repulsive quality of mutant prairie voles that could bias the behavior of potential partners, we developed a three-chamber assay that is a modified PPT but using all naive animals[16]. To ask this specific question about the *Scn2a*$^{\Delta 1a/+}$ voles, I tethered a naive, adult *Scn2a*$^{\Delta 1a/+}$ male or female vole in one chamber, and a sex-matched, age-matched, naive unrelated WT sibling (i.e., a littermate from a separate *Scn2a*$^{\Delta 1a/+}$ pair than produced the *Scn2a*$^{\Delta 1a/+}$ animal) in the other chamber, and allowed a naive, adult opposite-sex WT vole from a wildtype pair move freely between the chambers for 6 hours while being recorded. We can expect from previous experiments that each freely moving WT animal will spend a majority of the assay time with one of the tethered animals, designated the MOAT (More Over Assay Time), and we can rely on this to determine if there is a bias such that an opposite-sex conspecific preferentially spends time with one genotype over the other.

The videos from these assays were scored with automated contour tracking, which resulted in location data (in which chamber the freely moving animal was located across assay time) and contact data (onset time and duration of vole contours merging). Contact time does not get more granular than whether the contours are merged, such that nose touches to any part of the body, side-by-side huddles, and even agonistic tussles would all be labeled as a “contact”; however, known aspects of vole behavior would suggest that the bulk of “contact time” is affiliative in nature.

After analyzing the chamber location and durations, as well as contact time location and durations, we found that there was no bias in time spent near or in contact with either genotype. Specifically, when looking at chamber time, there is no significant difference between the overall time spent in the *Scn2a*$^{\Delta 1a/+}$ chamber or the WT sibling chamber at a population level, both when the freely moving animal is a WT male and WT female (Fig. 6A). There is also no significant difference between time spent in contact with either genotype at a population level for both males and females (Fig. 6B). When looking at preference index [(WT Contact time - *Scn2a*$^{\Delta 1a/+}$)/(Total

Contact Time)], we did observe that some WT males and WT females did develop a preference over the course of the six hours, though not all did, but the distribution of preferences is such that there is not a significant difference in either group (Fig. 6C). Therefore, we are able to conclude that there are no inherent qualities in the *Scn2a*$^{\Delta 1a/+}$ voles that impacts the behavior of WT animals in a biased way.

Vocal Behavior

Given that ASD diagnoses are typically characterized by communication differences in addition to social cognition and social behavior differences, we also wanted to assay ultrasonic vocalizations (USVs) of the *Scn2a*$^{\Delta 1a/+}$ voles as USVs are thought to be a form of communication/way to convey information from animal to animal in rodent species[18,19].

To achieve this, I paired an *Scn2a*$^{\Delta 1a/+}$ male with an unrelated *Scn2a*$^{\Delta 1a/+}$ female or a WT sibling male with an unrelated WT sibling female and recorded the pairs' vocalizations for 30 minutes. We cannot identify calls from individuals using the current setup in the lab, and so to determine the effects of *Scn2a* heterozygosity on vocalizations in an Introduction context, we must use genotype-matched pairs. I observed that the *Scn2a*$^{\Delta 1a/+}$ pairs vocalized significantly less over the course of the 30-minute recording such that there were significantly fewer USV calls compared to the WT sibling pairs (Fig. 7A). This appears to be a robust and non-specific effect as the phenotype is not dependent on assay time or due to a difference call duration distributions (Fig. 7B, D). Therefore, we can conclude that *Scn2a*$^{\Delta 1a/+}$ animals have a general deficit in USV calls compared to WT siblings. It will be important in the future to continue assaying dynamics of USVs in *Scn2a*$^{\Delta 1a/+}$ voles across various contexts and with mixed-genotype pairs to better understand if the phenotype persists across bonding stages and gain insights into whether the phenotype is driven by one sex or is sex specific. Despite there not being population differences in USV calls over assay time, it will also be informative to correlate USV call number, dynamics, and features to behavior by collecting video and microphone recordings simultaneously.

Stimulus-induced cFos expression in multiple contexts

Once I established a robust, and specific, behavioral phenotype in *Scn2a*$^{\Delta 1a/+}$ male prairie voles, the next step was to find neural correlates of these behaviors and behavioral differences. The first step I took towards achieving this was to do a whole-brain cFos screen. I started with just one behavioral assay, the Introduction assay, and modified the assay structure to optimize for cFos protein expression induced by the behavioral stimulus[20]. I chose the Introduction assay because that is the assay within the longitudinal battery that had several significant behavior differences between *Scn2a*$^{\Delta 1a/+}$ males and WT sibling males and therefore seemed to have a lot of potential for neural activation differences between the two groups, particularly in brain regions implicated in social behavior, such as the BNST, PFC, MeA, and LS. I only used males for these experiments because we did not find a female behavioral phenotype that would allow us to correlate neural differences to a specific behavior. There is of course the possibility that even in the absence of behavioral differences between *Scn2a*$^{\Delta 1a/+}$ females and WT female siblings that would indicate processing differences, but that would be a larger endeavor.

For this experiment, I adjusted the length of the assay from 30 minutes to 90 minutes to capture roughly 30 minutes of neural activation related-cFos expression in response to the novel female. Previous histology experiments in the Manoli lab have suggested that Ns of 3 per group are sufficient for finding statistically significant differences. Given the robustness of the behavioral phenotype in Introduction assay the longitudinal cohort of animals, I was confident that the new cohort of males would display comparable differences in affiliative behavior between the two genotypes that I did not record the behavior. After the 90-minute behavioral session where the *Scn2a*$^{\Delta 1a/+}$ male or WT sibling male was added to a fresh cage with a novel WT female, I performed transcardial perfusions on the male subject animals, dissected out the brain, and cryosectioned the tissue. For this experiment, I collected all sections from the brain beginning with the anterior PFC and ending just before the cerebellum. I then stained the tissue using a free-

floating section immunohistochemistry (IHC) with a monoclonal antibody conjugated to the cFos protein, a secondary fluorescent antibody for visualization, and DAPI. I then mounted the stained sections onto microscope slides for imaging. Using the Keyence BZ-X, I imaged every other section on the slide for the regions of interest: BNST, MeA, mPFC, and LS. The cFos staining lent itself to being counted using Fiji automated counting after thresholding, so I manually drew the regions of interest (ROI) for each nucleus on every section to be counted. I then normalized the automated count results for the area in microns of each ROI per section.

I analyzed the average of each section for each animal (Mann Witney), as well as analyzing each section as a data point (Linear Mixed Effects Model, random variable being animal ID). Neither analysis resulted in significant differences between groups (*Scn2a*$^{\Delta 1a/+}$ males vs. WT sibling males). This is likely due to the variation in phenotype - though many aspects of affiliative behaviors were significantly increased in the *Scn2a*$^{\Delta 1a/+}$ male group from the longitudinal cohort, it was not the case that every male displayed the exact same phenotype; rather, there was a heterogeneous mix of males that did not display uniform phenotypes on an individual level. In other words, some of the males displayed increased levels of anogenital sniffing, but not side-by-side huddling, and vice versa, and some males displayed both. Additionally, while the phenotype is robust, the affiliative behaviors are displayed by both groups, just more by the *Scn2a*$^{\Delta 1a/+}$ male more than their WT sibling males, potentially meaning this is not a sensitive enough assay to expose neural differences without temporal resolution. Therefore, this experiment was likely underpowered with N's of 3 and not optimized for uncovering cFos expression differences.

To address these caveats, I pivoted to a more optimal experiment that still aimed to find differences in cFos expression. The goal of the new experiment was to assay cFos expression differences after a bonded male (*Scn2a*$^{\Delta 1a/+}$ or WT sibling) was exposed to a novel naive female. This new design capitalized on prairie vole behavior and biology because "pair-bonded" (post sufficient cohabitation) is a vole-specific state, and therefore the social neural circuitry mediating the typical post-bonded behavior toward a novel female might be more sensitive and vulnerable

to perturbations such as *Scn2a* haploinsufficiency and therefore might allow for detectable differences in cFos expression. Additionally, the Stranger Rejection assay results suggested a more specific phenotype in the longitudinal male cohort such that there was a single behavior that was found to be significantly increased in the *Scn2a*$^{\Delta 1a/+}$ male population (side-by-side huddling), potentially resulting in more selective neural activation than found in the Introduction assay cFos screen. Furthermore, the baseline side-by-side huddling behavior found in WT sibling males is almost nonexistent, in that very few WT males show side-by-side huddling behavior with the naive female in this context, and those that do display the behavior do so at very low levels, as expected from known prairie vole behavior (REF). This again allowed us to hypothesize that this modified approach would be more sensitive and allow us to more easily detect differences in neural activation as quantified by cFos protein expression levels.

The modified experiment used the timing and structure of the normal Stranger Rejection assay, with an additional time period added to allow for cFos protein expression. Specifically, I started cohabitation of a naive adult *Scn2a*$^{\Delta 1a/+}$ male or WT sibling male with a naive adult unrelated WT female (Day 0). On Day 1, roughly 24 hours post-pairing, each pair was divided to induce estrus in the females while preventing mating to occur. On Day 2, another 24 hours later, the divider was pulled, and the cages were left in our housing room until Day 9, when I performed the behavioral assay and brain tissue collection. For this cohort of males, I did not run a partner preference test to check for the formation of a pair bond because there was not a correlation between preference index and Stranger Rejection huddle phenotype, which suggests that bonding status is not indicative of atypical Stranger Rejection behavior in *Scn2a*$^{\Delta 1a/+}$ males.

The Stranger Rejection Assay was modified to attempt to optimize cFos expression specifically in response to the introduction of and behavior toward/with the novel WT female. I first separated the *Scn2a*$^{\Delta 1a/+}$ male or WT sibling male from their cohabitated partner by removing the female from the home cage for 1 hour. I then added a novel WT female to the home cage of the male and recorded the behavior for 30 minutes. This is a deviation from the original assay, with

the purpose of inducing more cFos expression in the male brain from prolonged interaction with the female. I then divided the male from the stranger female using a transparent divider with small holes so the animals could no longer touch but are still able to perceive other sensory cues. I chose to divide the animals rather than separate them as isolation is very stressful to voles and I wanted to avoid cFos expression due to a stress response obscuring the cFos expression from the stranger stimulus. I then perfused the males with 4% PFA to fix the tissue and dissected out the brains. The brains were processed, sectioned, and stained using the same protocol and antibodies, and mounted as above. I again imaged the sections on the Keyence microscope and counted cFos puncta in the MeA, LS, and BNST of each animal using Fiji software (Fig. 8A). In addition to the neural cFos analysis, I also manually scored the behavior videos specifically for instances of side-by-side huddling behavior. This allowed me to define three distinct groups based on genotype and activity: WT sibling males (n=5), "Low-huddle" (LH) *Scn2a*$^{\Delta 1a/+}$ males (n=4), and "High-huddle" (HH) *Scn2a*$^{\Delta 1a/+}$ males (n=4) (Fig. 8B). I found no significant differences in cFos+ cell counts in the MeA, LS, or BNST between WT males, LH *Scn2a*$^{\Delta 1a/+}$ males, or HH *Scn2a*$^{\Delta 1a/+}$ males (Fig. 8C-E).

Discussion

Here I described the generation, validation, and behavioral characterization of prairie voles heterozygous for the ASD risk-associated gene, Scn2a. We successfully generated three unique alleles of the *Scn2a* locus, and we validated two of these alleles as loss of function mutations using electrophysiology. Lastly, we characterized the behavior of one of these mutant lines and found sex-specific and context-specific differences in adult attachment-related social behavior such that *Scn2a* haploinsufficiency in male prairie voles results in increases in affiliative behaviors regardless of context and identity of the stimulus animal in dyadic interactions, despite there being no observable differences in pair bond formation as shown by intact partner preference. We have thus established the prairie vole as a powerful model for studying developmental disorders

associated with social behavior differences, such as ASD, given that we are able to uncover social-specific differences in behavior in a heterozygous genetic model, results not often found in standard model organisms. From here, we can use *in vivo* neuroimaging techniques to potentially unmask neural- and circuit-level differences in these animals that correspond to these sex-specific behavioral phenotypes.

Our data support the notion that prairie vole pair-bonding behavior is modular[16]. Both males and females heterozygous for *Scn2a* display partner preference and aggressive stranger rejection after sufficient cohabitation, but *Scn2a* heterozygous males also display atypical affiliative behavior towards novel females both pre- and post-bonding with their cohabitated partner. Potentially this means that there are distinct circuits for these aspects of pair bonding, or that there is a separate affiliative circuit that functions independent of pair-bonding related circuitry and is selectively impacted by our *Scn2a* mutations. ASD is not typically thought of as an attachment disorder, and it is therefore not terribly surprising that we don't find attachment deficits in our model. Rather, the observed atypical social behavior may be related to a deficit in determining the appropriate social behavior given a specific context, a deficit that can be overcome by stronger partner recognition and preference. Now that we have characterized the specific social behavior phenotypes, we can begin to dissect out the circuitry and processing behind these behavioral differences in a mutant background, and potentially even in juxtaposition with other genetic models in the lab.

The male to female ratio of ASD diagnosis in humans is roughly 4:1[21,22]. Importantly, such sex differences are not explained by sex chromosomes. There are many hypotheses as to why this phenomenon occurs, such as increased male risk or a female protective effect[23]. Diagnostic criteria for many psychiatric disorders were developed based on studies that exclusively included males, which in turn means that female manifestation of ASD is not well understood. In other words, only relatively few females compared to males will present with the core symptoms outlined in the DSM or evaluated in the standard test for diagnosis, but there are potentially many

more females going undiagnosed because their symptoms manifest differently. Despite the lack of understanding and fundamental gaps in our knowledge, neurobiological research of these disorders is still often only done in males, leaving female neurobiology in the context of psychiatric disorders poorly understood, resulting in an incomplete understanding of many biological concepts. Thus, when modeling these neurological processes, disorders, and their associated phenotypes, we need to continue to examine both sexes, not necessarily to compare or highlight these differences but to take an unbiased approach to understanding the sexes independently of each other.

Materials & Methods

Animals: Subjects were laboratory-bred prairie voles (*Microtus ochrogaster*) which originated through systematic outbreeding of a wild stock captured near Champaign, Illinois. Sexually naïve male and female animals were group weaned at 21 ± 5 days separated to group housing with same-sex siblings and age-matched same-sex non-siblings. Voles were maintained under a 14:10 h light-dark cycle in clear plastic cages 673 (45 × 25 × 15 cm) with bedding, nesting material (nestlet), and a PVC hiding tube. Rooms were maintained at approximately 20°C, and food and water were available *ad libitum*.

Generation of Scn2a Heterozygous Mutants: Based on the sequences of *Scn2a* in the current assembly of the prairie vole genome, we designed sgRNAs targeting multiple exons in the gene.

Table 1: sgRNA sequences used for generation of $Scn2a^{-/+}$ vole lines.

sgRNA ID	Sequence	Source
Scn2a sg 1	CAGAAGAGAAAGCCAAGAGACCCAAAC	In house
Scn2a sg 2	CCAAGAGACCCAAACAGGAACGCA	In house
Scn2a sg 8	GAGATGGTGTCAGAGCCCCTGGAGGAC	In house
Scn2a sg 4	ATGGTGTCAGAGCCCCTGGAGGACC	In house
Scn2a sg 13	TAATCCTCCAGACTGGACAAAGAATG	In house

Embryo harvesting: Methods described previously[17]. Briefly, adult male and female prairie voles were paired and put through a timed mating protocol to induce estrus and yield time-locked fertilization. Embryos were then harvested from the females.

Electroporation: We performed electroporation of the sgRNA guides, Cas9 protein, and cas9 mRNA on embryos and cultured the manipulated embryos to the blastocyst stage. We generated pseudopregnant recipient females using our timed mating protocol with vasectomized males and surgically implanted the manipulated embryos into their oviduct. Using such an approach, we developed a protocol whereby 10 embryos are transferred to each uterine horn to obtain 3-5 live born pups per female.

PCR and Sequencing Confirmation: Mutations were characterized using PCR and confirmed using sequencing. Three mutations were identified: a 108 base pair deletion in exon 1 (Exon1a), a 12 base pair deletion in exon 1 (Exon1b), and a 2 base pair deletion in exon 3. The Exon1b mutation was extremely difficult to genotype, so we therefore cataloged the mutation and discontinued the breeding of this line. We the crossed our mutant voles to at least 7 generations of outcrosses isolate the mutations in *Scn2a* from any off-target events due to CRISPR-mediated mutagenesis[17]. Each animal from litters used for behavior experiments was genotyped from a tail sample collected upon weaning and the genotype was confirmed with a tail sample collected after euthanasia post-experiment. If these genotypes were not in consensus, the animal was excluded from analysis.

Primers:

exon 1a primers – F: AGGGAATCCCTTGCTGCTATTG; R: ATATAGTAGGGGTCCAGGTCC;

Sequencing primer: TGCTGACTTTGTTTTCCTTGACA

Exon 3 primers – F: TTAGTGGGGTGAAGACAGGG; R: TCGCCACAACATGCAGAAC;

Sequencing primer: AAGGCAGGCTCAAACAAGTG

Ex Vivo Electrophysiology: Voles aged P25 through P30 were anesthetized, and 250 µm-thick coronal slices containing medial prefrontal cortex were prepared. Slices were prepared from *Scn2a*$^{+/-}$ or *Scn2a* wild-type littermates (genotyped by PCR). All data were acquired and analyzed blind to *Scn2a* genotype. Data were acquired from both sexes (blind to sex), with no sex-dependent differences noted in measurements made in acute slice recordings. Cutting solution contained (in mM): 87 NaCl, 25 $NaHCO_3$, 25 glucose, 75 sucrose, 2.5 KCl, 1.25 NaH_2PO_4, 0.5 $CaCl_2$ and 7 $MgCl_2$; bubbled with 5%CO_2/95%O_2; 4°C. Following cutting, slices were incubated in the same solution for 30 min at 33°C, then at room temperature until recording. Recording solution contained (in mM): 125 NaCl, 2.5 KCl, 2 $CaCl_2$, 1 $MgCl_2$, 25 $NaHCO_3$, 1.25 NaH_2PO_4, 25 glucose; bubbled with 5%CO_2/95%O_2; 32-34°C, ~310 mOsm.

Neurons were visualized with differential interference contrast (DIC) optics for conventional visually guided whole-cell recording. For current-clamp recordings, patch electrodes (Schott 8250 glass, 3-4 MΩ tip resistance) were filled with a solution containing (in mM): 113 K-Gluconate, 9 HEPES, 4.5 $MgCl_2$, 0.1 EGTA, 14 $Tris_2$-phosphocreatine, 4 Na_2-ATP, 0.3 tris-GTP; ~290 mOsm, pH: 7.2-7.25. All data were corrected for measured junction potentials of 12.

Electrophysiological data were acquired using Multiclamp 700A or 700B amplifiers (Molecular Devices) via custom routines in IgorPro (Wavemetrics). For measurements of action potential waveform, data were acquired at 50 kHz and filtered at 20 kHz. For current-clamp recordings, pipette capacitance was compensated by 50% of the fast capacitance measured under gigaohm seal conditions in voltage-clamp prior to establishing a whole-cell configuration, and the bridge was balanced. Series resistance was < 15 MΩ in all recordings. Experiments were omitted if input resistance changed by > ± 15%.

Recordings were restricted to L5b. In pyramidal cells aged > P17, AP characteristics are known to vary based on cell class[24,25]. To minimize variability, recordings were restricted to L5b cells with high HCN expression levels, corresponding to pyramidal tract (PT) neurons. In current

clamp, PT neurons were defined as those that exhibited a voltage rebound more depolarized than V_{rest} following a strong hyperpolarizing current (−400 pA, 120 ms) that peaked within 90 ms of current offset[24]. AP threshold and peak dV/dt measurements were determined from the first AP evoked by a 300 pA current in pyramidal cells (300 ms duration). Threshold was defined as the V_m when dV/dt measurements first exceeded 15 V/s.

Behavior: We used a version of sensitized behavioral battery to assess adult attachment behavior[16]. The timeline of these behaviors can be found in Figure 3.

Introduction - The subject animal is paired with a WT, opposite-sex stranger in a Thoren cage and recorded for 30 minutes. 24 hours after this assay, animals within a pair will be separated within their home cage by a divider, allowing for nose-to-nose interaction, but not mating, to induce estrus in the female animal.

Timed mating - Divider is removed and behaving pairs are recorded for 30 minutes in their home cage.

Partner preference test (PPT) - The cohabitated partner of the subject animal is tethered in one chamber and an opposite-sex stranger is tethered on the other side of a three-chamber apparatus lined with their normal home cage bedding such that they each can move within their respective chamber, but not to the other center or other side. Dividers are placed before the assay starts to block off the left and right chambers and the subject animal is placed into the center chamber. The assay begins when the dividers are removed from the lane, and the behavior is recorded for 3 hours as the animal moves freely between the three chambers.

Partner Reunification - The cohabitated partner animal is removed from the home cage for 60 minutes, while the subject is left alone in the home cage for this time period, which is recorded but not scored. After 60 minutes, the partner is returned to the home cage and reunited with the subject animal; this portion of the assay is recorded for 30 minutes.

Stranger Rejection - The cohabitated partner animal is removed from the home cage for 60 minutes, while the subject is left alone in the home cage for this time period, which is recorded but not scored. An opposite-sex, naive stranger animal will be added to the home cage of the subject animal and behavior is recorded for 20 minutes. In order to prevent excessive aggressive behavior bouts, the experimenter remains in the room during the assay and will remove the stranger animal if 3 bouts of tussling occur, and the subject animal will be excluded from the analysis of this assay.

We also conducted a series of 2 control behavior assays to test for anxiety and locomotion phenotypes. The control assays are conducted using an independent cohort from the attachment behavior cohort and run such that each animal in the cohort did the open field test (OFT) 48 hours after the three-chamber test (TCT).

Sociability TCT - Subject animals were placed in a three-chamber lane and habituated to the apparatus for 10 minutes. Subject animals were then restrained to the center chamber by the addition of dividers. A novel, naive, sex-matched animal was added to one chamber under a cup and weights to prevent escape, and a wooden block is placed under a cup and weights in the opposite chamber. The dividers are then removed, and the animal is allowed to explore each chamber freely for 10 minutes.

OFT - Our lab created a custom open field apparatus designed in-house for prairie voles. The subject animal was habituated to the arena for 10 minutes and then recorded for 10 minutes.

Naïve Choice – This assay was conducted as previously described[16]. Briefly, two same-sex naïve prairie voles were tethered to either side of a three-chamber apparatus, and one opposite-sex prairie vole was placed into the center chamber with the ability to freely move throughout all three chambers. The assay was run and recorded for 6 hours. Lanes that included animals that became de-tethered at some point during the 6-hour assay were excluded from analysis.

Vocalization behavior - Non-related adult, naïve male *Scn2a*$^{\Delta 1a/+}$ voles or WT sibling voles were removed from their group housing cages and placed into a clean Thoren cage in a sound box

equipped with a home cage-top camera and microphone setup for video and audio recording for 5 minutes. A genotype-matched, age-matched female vole was then introduced to the cage and the pair were left to interact for 30 minutes while the behavior and vocalizations were recorded. Recordings are captured while pairs of voles interact freely in a home cage placed in a sound insulating chamber to prevent audio bleed between simultaneous recordings. A single free-field microphone (Noldus Information Technology Inc., Leesburg, VA) is suspended 6 inches above the center of the home cage and the cage is illuminated from the same plane as the microphone using a custom apparatus that fits atop the home cage. Audio files are recorded at a sampling rate of 250 kHz using UltraVox software (Noldus Information Technology Inc., Leesburg, VA). Audio recordings are automatically segmented using a vak vocalization detection network trained on 6700 s of manually annotated prairie vole vocalizations[26]. The output of the network is an annotation of times during which vocalization is occurring. Windows during which vocalization is annotated as occurring are designated as putative calls and used for further analysis. The putative calls are time-aligned to the start of the assay. The assay consists of introducing a male to a clean home cage. After the male has explored the home cage for five minutes, an age- and genotype-matched female is introduced to the cage. The addition of the female to the cage constitutes the assay start time (0 s). Putative calls are analyzed for the following 1800 s. The number, duration, and time of occurrence of annotations corresponding to putative calls recorded per pair are tabulated with custom Python software. Non-parametric tests are used for statistical comparisons. Histograms are computed using 30-second bins.

Immunohistochemistry (IHC): Scn2a$^{\Delta 1a/+}$ male or WT sibling male voles were either run through an Introduction Assay or modified Stranger Rejection Assay before perfusion. Each animal was perfused transcardially with 25mL ice cold phosphate buffer (PBS) and fixed in 25mL of 4% paraformaldehyde in PBS (PFA). Whole brain was dissected and post fixed overnight at 4°C in 4% PFA in the dark. The tissue was cryoprotected for 24 hours in 30% sucrose in PBS and then

embedded in OCT over dry ice to prevent cracking. 50µm serial sections from the entire PVN were collected in PBS and processed as free-floating sections. Sections were blocked using 10% donkey serum in 0.1% Triton X 100 in PBS and then stained with primary antibodies (cFos Monoclonal Antibody, Synaptic Systems, Rat Monoclonal, Cat #226017, 1:5000) in 1% donkey serum with 0.1% Triton X 100 (staining buffer) in PBS at 4°C with shaking. The sections were rinsed and soaked in secondary antibodies (Cy™3 AffiniPure Donkey Anti-Rat IgG, Jackson ImmunoResearch Laboratory, Cat #711-165-150, 1:500) in staining buffer for 2 hours at room temperature. Sections were DAPI stained and transferred to glass slides in sequence and mounted in DABCO. Slides were imaged using a fluorescent microscope (Keyence-BZ) and the puncta in a hand-drawn ROI were quantified in ImageJ. Comparisons of cell density (count/area) were made in age and sex matched samples.

Scoring: Adult attachment behavior used the BORIS software for manual scoring by individuals. Each assay was scored by a single individual to maintain within-assay consistency. We developed ethograms for home cage assays (Introduction, Timed Mating, Partner Reunification, Stranger Rejection) and for the PPTs. These ethograms each contain a range of affiliative and agonistic behaviors, that can be coded to have a duration (state event) or have a single time-stamp and no duration (point event) The ethogram used for scoring the home cage behaviors included state events (non-anogenital sniffing, anogenital sniffing, side-by-side huddling, no interaction, mounting, intromission, defensive rear and tussle) and point events (strike, defensive strike, ejaculation, and aggression received). The PPT ethogram included chamber location (left, center, and right), interact left and interact right (nose-touch to any part of the tethered animal's body), and huddle left and huddle right, all state events. The PPT ethogram also included point events for aggression left or aggression right, coding for agonistic behaviors instigated by the freely moving subject animal toward the tethered stimulus animals. Control behaviors and Naïve Choice assays were scored with animated contour tracking developed in-house.

Data Analysis: Prism or python. If data were normal, t-tests were used. When the data were log-normal, the data were log transformed, and t-tests were run on the then log normal data. If data were not normal or log-normal, Mann-Whitney tests were used for analysis. For PPTs comparing multiple groups (chamber time and huddle time for each sex), I used Mixed-effects analysis with Bonferroni correction for multiple comparisons.

Figures

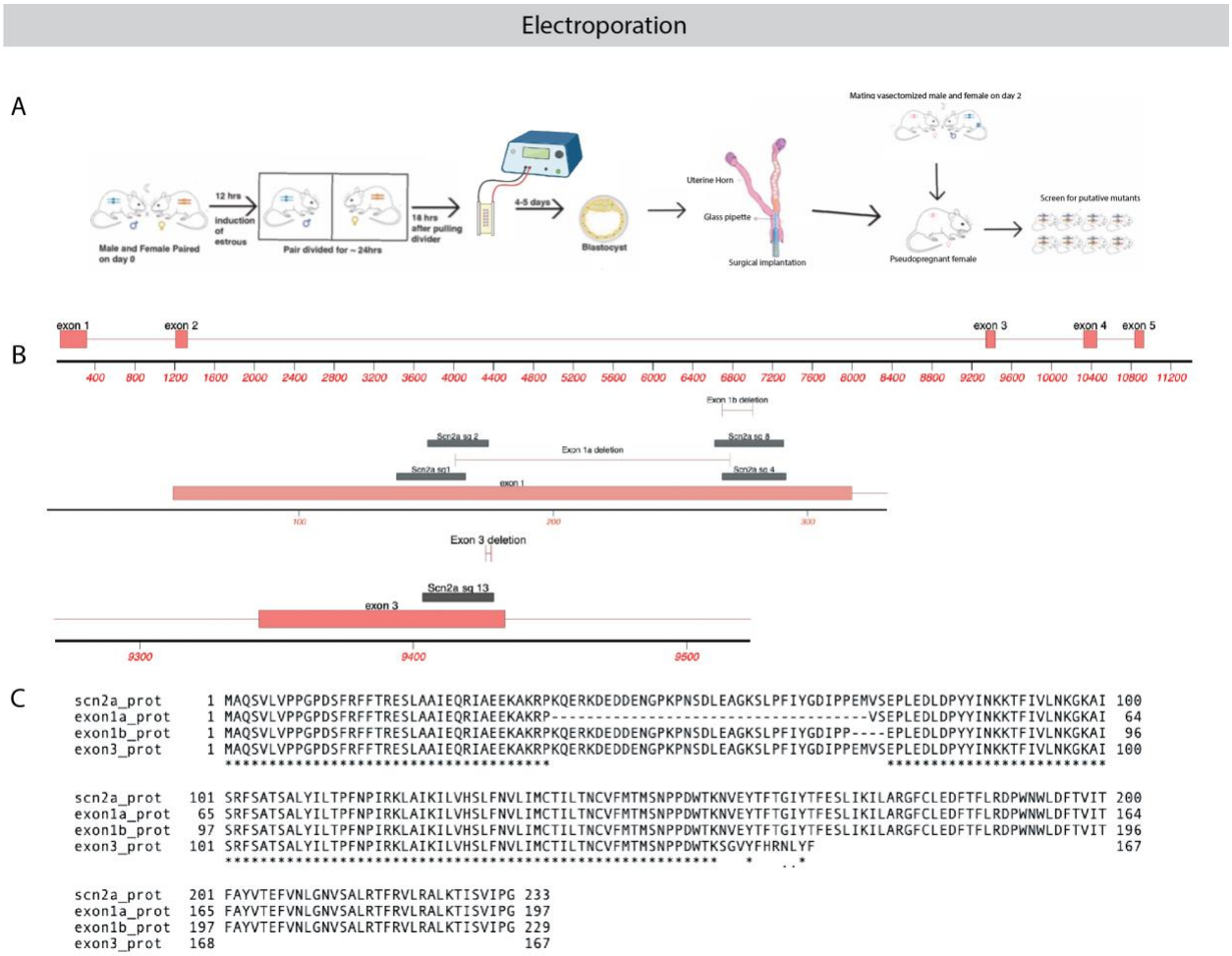

Figure 1: Generation and molecular validation of *Scn2a* heterozygous mutant prairie voles.

A. Schematic depicting our electroporation protocol.
B. Map of the first 5 exons of the prairie voles *Scn2a* locus (top) and the location of the guide RNAs and subsequent mutations found in exon 1 (middle) and exon 3 (bottom).
C. Protein alignments of the full *Scn2a* locus, the exon 1a in-frame deletion, the exon 1b in-frame deletion, and the protein-truncating exon 3 deletion.

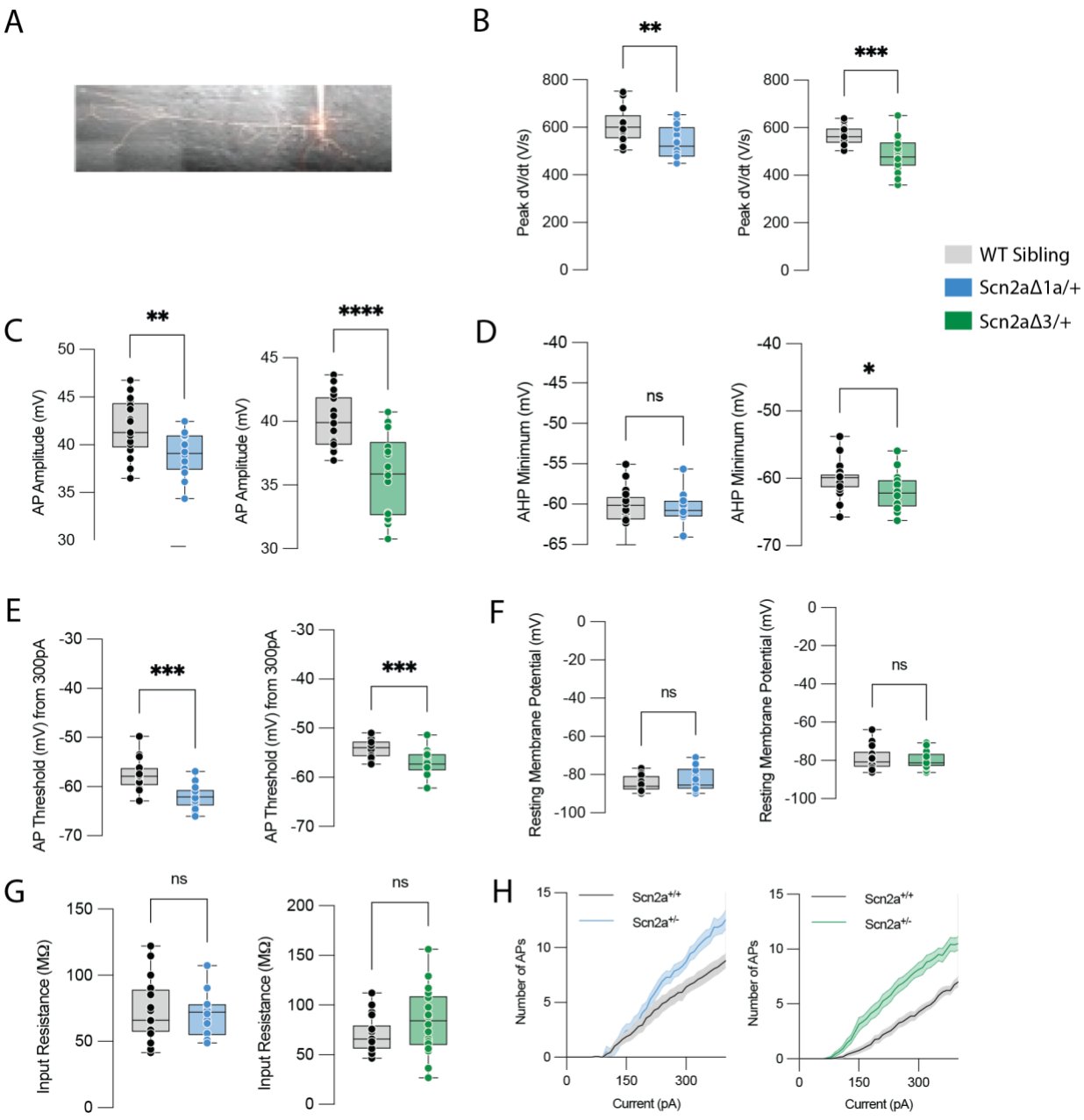

Figure 2: Whole-cell current-clamp electrophysiology validation of loss of function of Exon 1a and Exon 3 deletions.

A. Example image of the whole-cell current clamp approach in the prefrontal cortex (PFC).
B. Peak dV/dt of action potentials is significantly decreased in Exon$^{\Delta 1a/+}$ cells (left) and Exon$^{\Delta 3/+}$ cells (right) compared to WT siblings.
C. Action potential amplitude is significantly decreased in Exon$^{\Delta 1a/+}$ cells (left) and Exon$^{\Delta 3/+}$ cells (right) compared to WT siblings.

(Figure caption continued on the next page.)

(Figure caption continued from the previous page.)

D. After hyperpolarization (AHP) minimum following action potential is not different in Exon$^{\Delta 1a/+}$ cells compared to WT siblings (left). AHP minimum following action potential is significantly decreased in Exon$^{\Delta 3/+}$ cells compared to WT siblings (right).
E. Action potential threshold is significantly decreased in ExonΔ1a/+ cells (left) and Exon$^{\Delta 3/+}$ cells (right) compared to WT siblings.
F. Resting membrane potential is not different in Exon$^{\Delta 1a/+}$ cells (left) or Exon$^{\Delta 3/+}$ cells (right) compared to WT siblings.
G. Input resistance is not different in Exon$^{\Delta 1a/+}$ cells (left) or Exon$^{\Delta 3/+}$ cells (right) compared to WT siblings.
H. The number of action potentials increase with increasing current in both Exon$^{\Delta 1a/+}$ cells (left) and Exon$^{\Delta 3/+}$ cells (right) compared to WT siblings.

[For all plots: Exon 1a WT siblings n=19 cells, Exon$^{\Delta 1a/+}$ n = 14 cells; Exon 3 WT siblings n=18 cells, Exon$^{\Delta 3/+}$ n=19 cells; Mann Whitney, ns not significant, **p<0.01, ***p<0.001. ****p<0.0001]

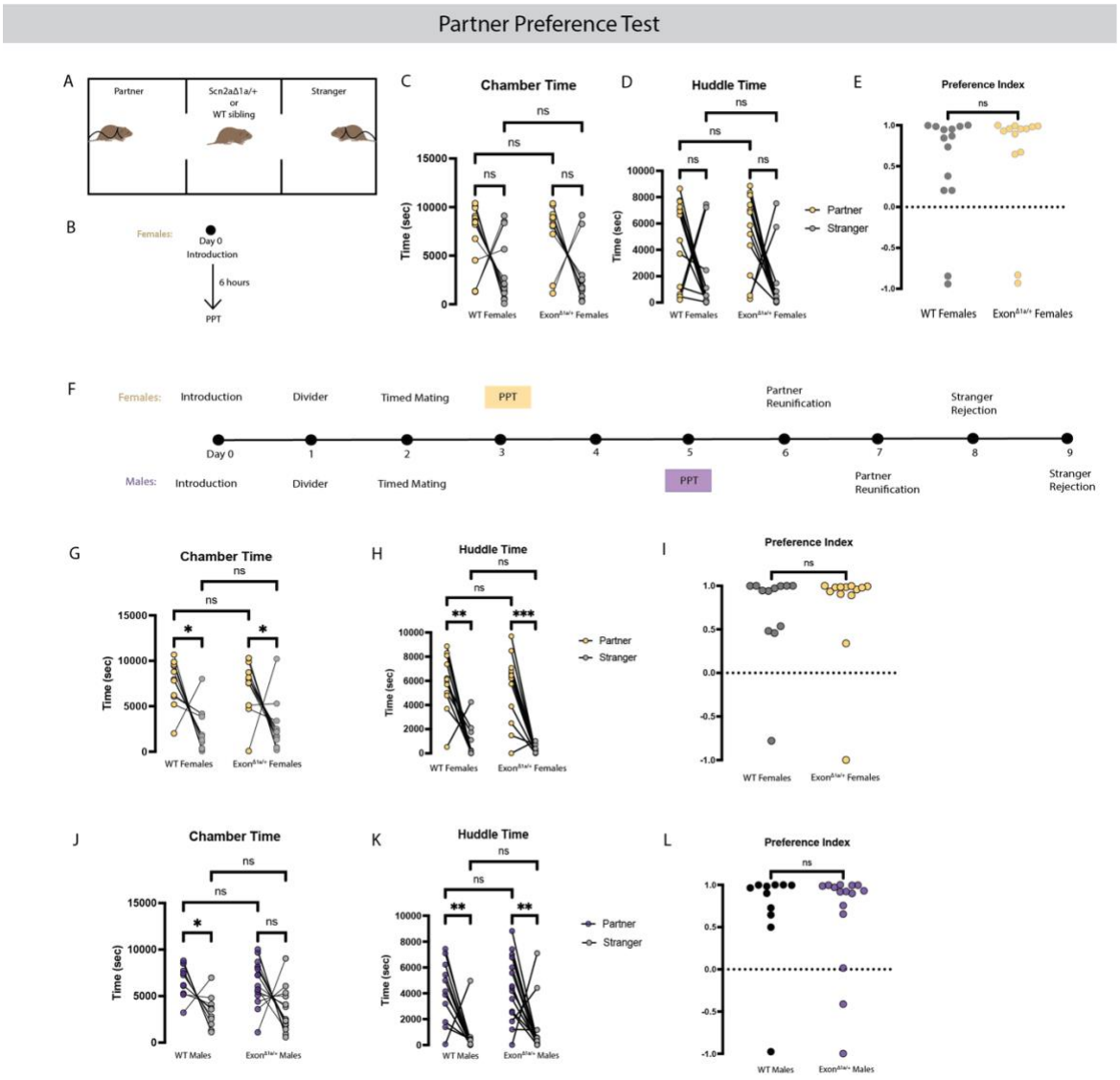

Figure 3: $Na_V1.2$ haploinsufficiency does not impact partner preference after sufficient cohabitation.

A. Cartoon of the partner preference test (PPT) setup.
B. Timeline of 6-hour cohabitation cohort of female voles.
C. No significant difference in time spent in the partner chamber (yellow) or stranger chamber (gray) in WT sibling females or in *Scn2a*$^{\Delta 1a/+}$ females after 6 hours of cohabitation, and no significant difference between the two groups in time spent in the partner chamber or stranger chamber. [Mixed-effects model, ns not significant].
D. No significant difference in time spent huddling with the partner (yellow) or stranger (gray) in WT sibling females or in *Scn2a*$^{\Delta 1a/+}$ females after 6 hours of cohabitation, and no significant difference between the two groups in time spent engaged in a side-by-side huddle with the partner or stranger. [Mixed-effects model, ns not significant].

(Figure caption continued on the next page.)

(Figure caption continued from the previous page.)

E. Partner preference indexes (PPI) [(partner huddle time - stranger huddle time)/(total huddle time)] of WT sibling females and *Scn2a*$^{\Delta 1a/+}$ females do not significantly differ after 6 hours of cohabitation with a male partner. PPI > 0 = partner preferring; PPI < 0 = stranger preferring. [Mann Whitney, ns not significant].
F. Longitudinal timeline used for male and female cohorts that went through the full adult attachment behavior battery. PPTs occur 24 hours after the Timed Mating assay in females (Day 3) and 72 hours after the Timed Mating assay in males (Day 5).
G. Significant increase in time spent in the partner chamber (yellow) compared to the stranger chamber (gray) in WT sibling females and in *Scn2a*Δ1a/+ females, but no significant difference between the two groups in time spent in the partner chamber or stranger chamber. [Mixed-effects model, ns not significant, *p<0.05].
H. Significant increase in time spent in a side-by-side huddle with the partner (yellow) compared to the stranger (gray) in WT sibling females and in *Scn2a*$^{\Delta 1a/+}$ females, but no significant difference between the two groups in time spent engaged in a side-by-side huddle with the partner or stranger. [Mixed-effects model, ns not significant, **p<0.01, ***p<0.001].
I. PPI of WT sibling females and *Scn2a*$^{\Delta 1a/+}$ females do not significantly differ after 48 hours of cohabitation with a male partner. [Mann Whitney, ns not significant].
J. Significant increase in time spent in the partner chamber (purple) compared to the stranger chamber (gray) only in WT sibling males but not in *Scn2a*$^{\Delta 1a/+}$ males. No significant difference between the two groups in time spent in the partner chamber or stranger chamber. [Mixed-effects model, n.s not significant, *p<0.05].
K. Significant increase in time spent in a side-by-side huddle with the partner (purple) compared to the stranger (gray) in WT sibling males and in *Scn2a*$^{\Delta 1a/+}$ males, but no significant difference between the two groups in time spent engaged in a side-by-side huddle with the partner or stranger. [Mixed-effects model, ns not significant, **p<0.01].
L. PPI of WT sibling males and *Scn2a*$^{\Delta 1a/+}$ males do not significantly differ after 120 hours of cohabitation with a female partner. [Mann Whitney, ns not significant].

[Day 0 PPT Cohort: WT Females n = 14, *Scn2a*$^{\Delta 1a/+}$ Females n = 12; Longitudinal Cohort: WT Females n = 13, *Scn2a*$^{\Delta 1a/+}$ Females n = 13, WT Males = 12, *Scn2a*$^{\Delta 1a/+}$ Males n = 15]

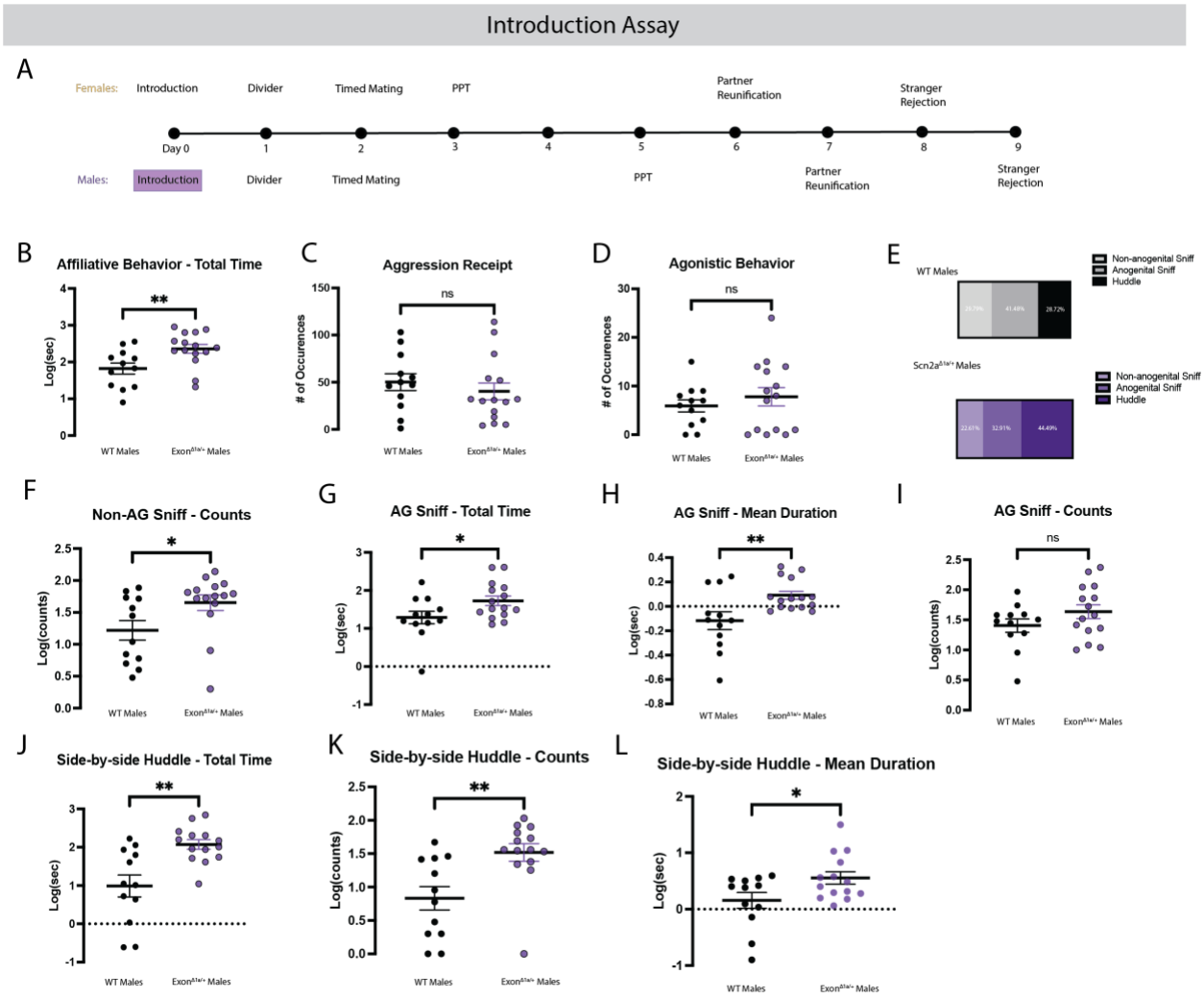

Figure 4: $Na_V1.2$ haploinsufficiency leads to increased affiliative behavior in male prairie voles during initial interactions.

A. Male and female introductions occur on Day 0 of the longitudinal timeline.
B. Total time spent engaged in affiliative behavior with the naive female during the Introduction assay is increased in *Scn2a*$^{\Delta 1a/+}$ males compared to WT sibling males.
C. No significant difference in the frequency of aggressive behavior directed toward the subject male by the naive female vole between *Scn2a*$^{\Delta 1a/+}$ males compared to WT sibling males.
D. No significant difference in the frequency of agonistic behaviors directed towards the naive female between *Scn2a*$^{\Delta 1a/+}$ males compared to WT sibling males.
E. Proportion of time spent engaged in each of the affiliative behaviors (non-anogenital sniffs, anogenital sniffs, and side-by-side huddles) in WT sibling males (top) and *Scn2a*$^{\Delta 1a/+}$ males (bottom). 100% = total time engaged in affiliative behavior.
F. *Scn2a*$^{\Delta 1a/+}$ males display a significantly increased number of non-anogenital (AG) sniffs of the naive female compared to WT male siblings.

(Figure caption continued on the next page.)

(Figure caption continued from the previous page.)

G. *Scn2a*$^{\Delta 1a/+}$ males display significantly increased total time engaged in AG sniffs of the naive female compared to WT male siblings.
H. *Scn2a*$^{\Delta 1a/+}$ males display significantly increased mean duration of AG sniff bouts of the naive female compared to WT male siblings.
I. *Scn2a*$^{\Delta 1a/+}$ males display a significantly increased number of (AG) sniffs of the naive female compared to WT male siblings.
J. *Scn2a*$^{\Delta 1a/+}$ males display significantly increased total time engaged in side-by-side huddles with the naive female compared to WT male siblings.
K. *Scn2a*$^{\Delta 1a/+}$ males display a significantly increased number of side-by-side huddles with the naive female compared to WT male siblings.
L. *Scn2a*$^{\Delta 1a/+}$ males display significantly increased mean duration of bouts of side-by-side huddling with the naive female compared to WT male siblings.

[B, F-L: All data shown were log normal and log transformed, then an unpaired t-test was used to test significance; ns not significant, *$p<0.05$, **$p<0.01$. C-D: Mann Whitney tests, ns not significant. WT Females n = 13, *Scn2a*$^{\Delta 1a/+}$ Females n = 13, WT Males = 12, *Scn2a*$^{\Delta 1a/+}$ Males n = 15]]

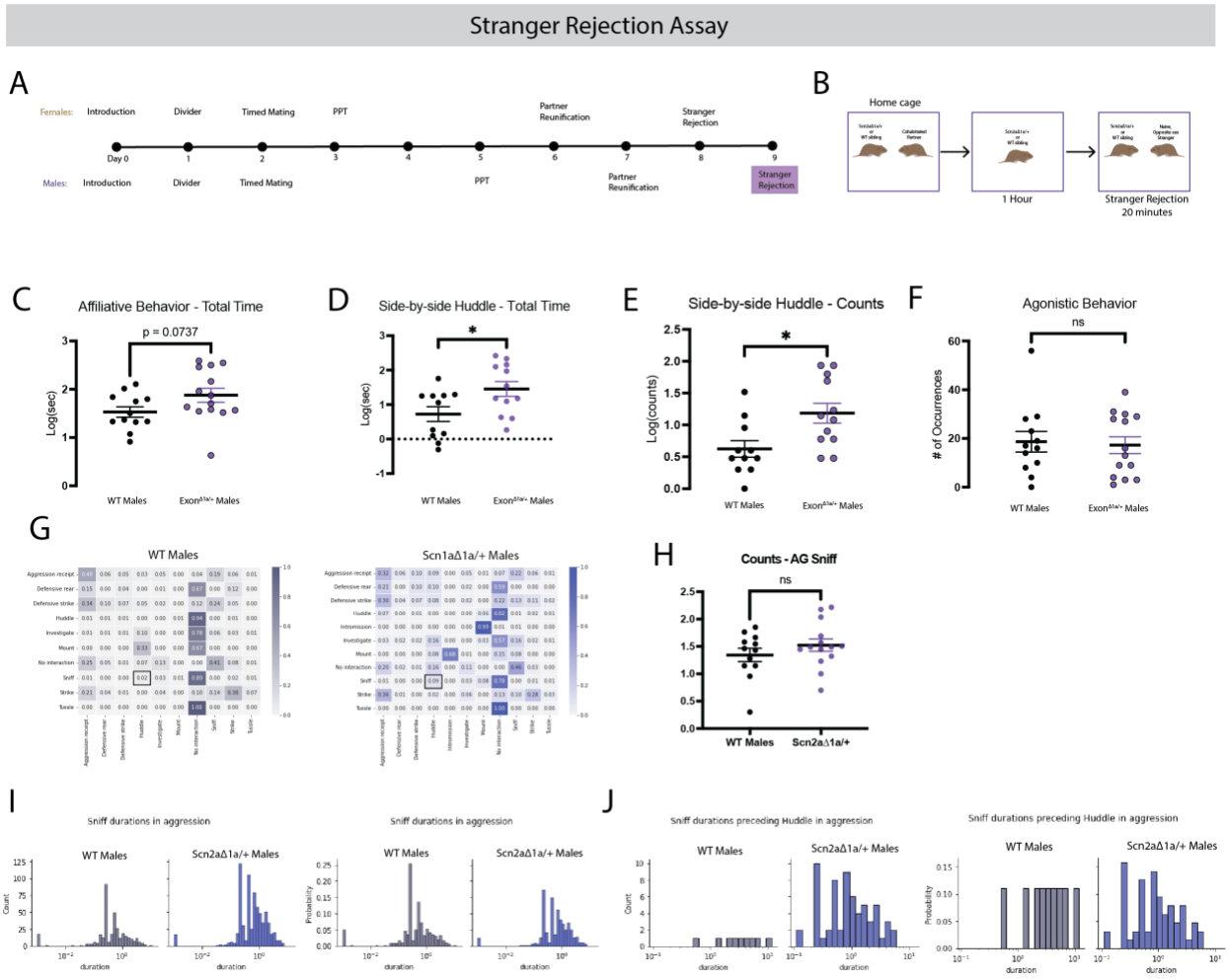

Figure 5: $Na_V1.2$ haploinsufficiency induces exploration and affiliation with a stranger female, but does not decrease aggression, in pair-bonded male prairie voles.

A. Stranger Rejection assay occurs on Day 9 of the longitudinal timeline for male prairie voles.
B. Schematic describing the Stranger Rejection assay experimental set up.
C. Increased total time engaged in affiliative behavior with the stranger female by *Scn2a*$^{\Delta 1a/+}$ males compared to WT sibling males is trending, but not significant.
D. *Scn2a*$^{\Delta 1a/+}$ males display significantly increased total time engaged in side-by-side huddles with the stranger female compared to WT male siblings.
E. *Scn2a*$^{\Delta 1a/+}$ males display a significantly increased number of side-by-side huddles with the stranger female compared to WT male siblings.
F. No significant difference in the frequency of agonistic behaviors directed towards the stranger female between *Scn2a*$^{\Delta 1a/+}$ males compared to WT sibling males.

(Figure caption continued on the next page.)

(Figure caption continued from the previous page.)

G. Markov chain transition matrices for all behaviors in the Stranger Rejection assay for WT sibling males (left) and *Scn2a*$^{\Delta 1a/+}$ males (right). Column behavior precedes row behavior. Boxed values are specifically highlighting the proportion of sniffs that transition into a huddle. [63/712 or 9% in *Scn2a*$^{\Delta 1a/+}$ males vs. 9/363 or 2% in WT sibling males, Chi-squared p-value = 0.00013]
H. No statistical difference in the frequency of AG sniffs of the stranger female between *Scn2a*$^{\Delta 1a/+}$ males compared to WT sibling males.
I. Histogram depicting the frequency (left) and probability (right) of AG sniffs by duration in WT sibling males and *Scn2a*$^{\Delta 1a/+}$ males.
J. Histogram depicting the frequency (left) and probability (right) of AG sniffs that precede a huddle by duration in WT sibling males and *Scn2a*$^{\Delta 1a/+}$ males.

[C-E, H: All data shown were log normal and log transformed, then an unpaired t-test was used to test significance; ns not significant, *p<0.05, **p<0.01. WT Females n = 13, *Scn2a*$^{\Delta 1a/+}$ Females n = 13, WT Males = 12, *Scn2a*$^{\Delta 1a/+}$ Males n = 15]

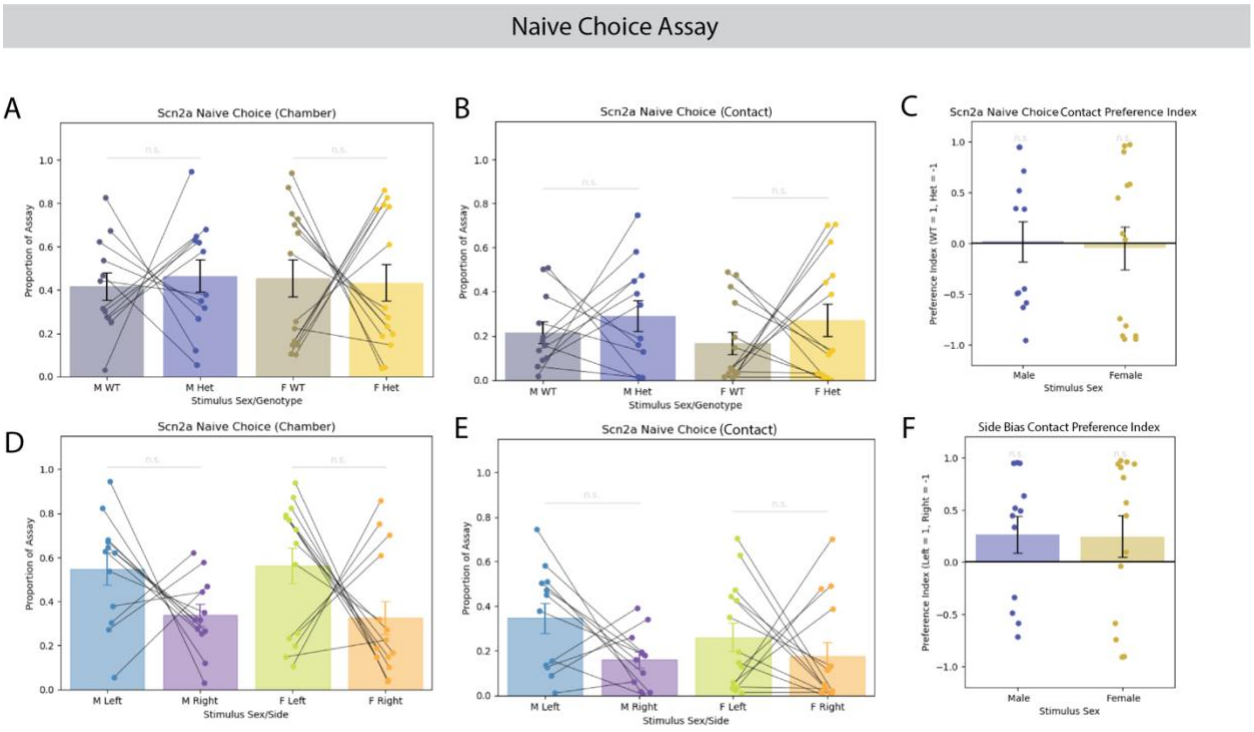

Figure 6: *Scn2a* heterozygosity does not bias the behavior of WT opposite-sex animals.

A. There is no significant difference in time spent by WT male or female prairie voles in the chamber of opposite-sex *Scn2a*$^{\Delta 1a/+}$ or WT sibling voles.
B. There is no significant difference in time spent by WT male or female prairie voles in contact with opposite-sex *Scn2a*$^{\Delta 1a/+}$ or WT sibling voles.
C. The average preference index of male and female WT voles is not significantly different than 0 such that there is no preference for one genotype or the other.
D. Neither male nor female WT voles display a preference for one side of the three chamber apparatus when looking at time spent in either chamber.
E. Neither male nor female WT voles display a preference for spending time contacting another animal on one side of the three chamber apparatus.
F. The average preference index of male and female WT voles is not significantly different than 0 such that there is no preference for one chamber side over the other.

[Male Choosing Lanes n = 14, Female Choosing Lanes n = 12. A-B, D-E: Wilcoxon signed-rank test; C, F: 1-sample t-tests. n.s. = not significant]

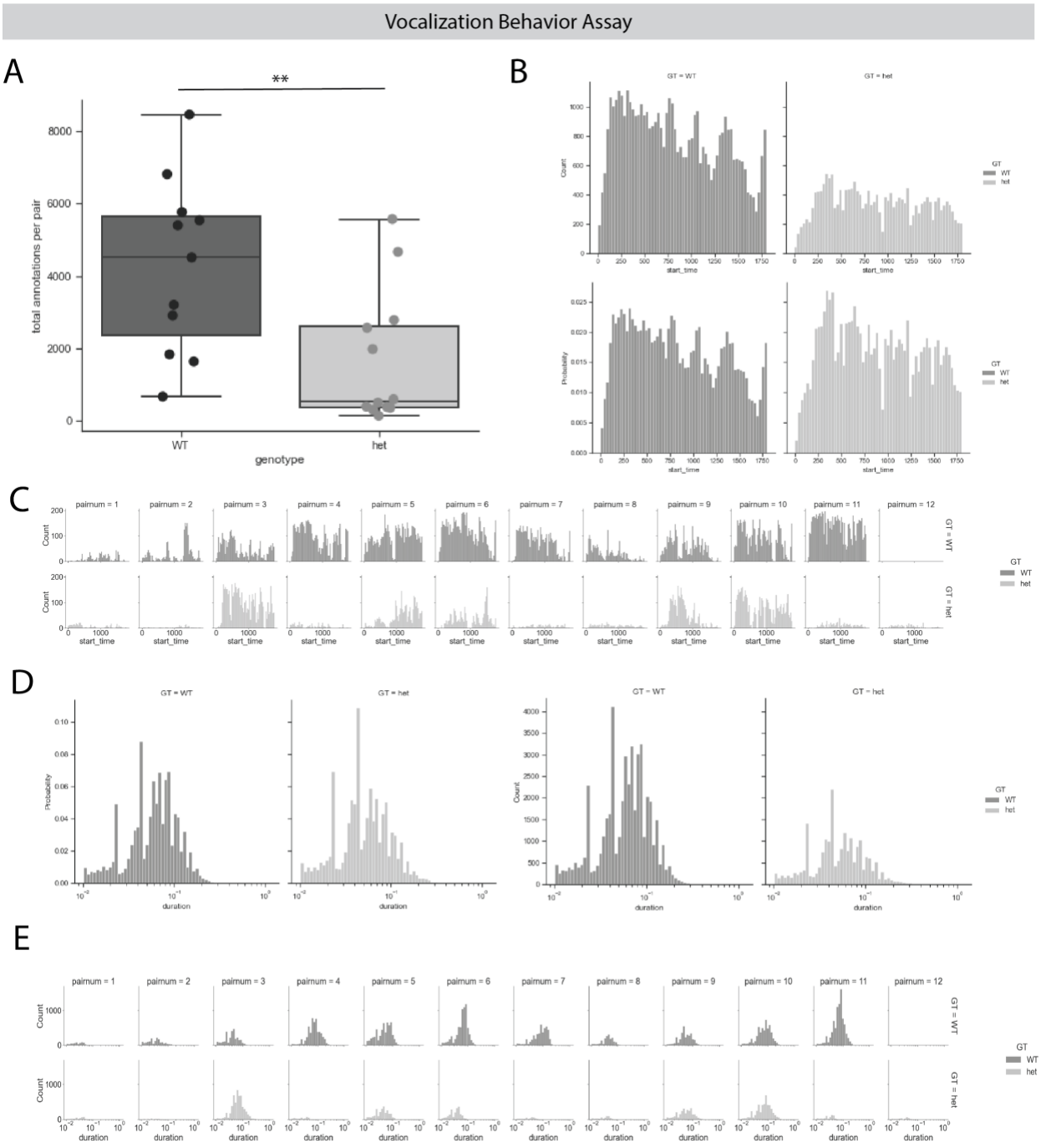

Figure 7: Pairs of *Scn2a*$^{\Delta 1a/+}$ vocalize less during initial interactions than WT pairs.

A. *Scn2a*$^{\Delta 1a/+}$ pairs call less than WT pairs of voles during a 30-minute introduction period as shown by a significant decrease in total call number.

B. There is no difference in call distribution over assay time between WT pairs and *Scn2a*$^{\Delta 1a/+}$ pairs. Top – raw counts; bottom – probability metric normalized by total calls.

C. Individual pair distributions of calls by assay time (raw counts) for WT pairs (top) and *Scn2a*$^{\Delta 1a/+}$ pairs (bottom) highlighting variability of call number within a genotype.

(Figure caption continued on the next page.)

(Figure caption continued from the previous page.)

D. Distribution of call durations are not different between WT pairs and *Scn2a*$^{\Delta 1a/+}$ pairs. Left– raw counts; right – probability metric normalized by total calls.

E. Individual pair distributions of call durations (raw counts) for WT pairs (top) and *Scn2a*$^{\Delta 1a/+}$ pairs (bottom) highlighting variability of call number within a genotype.

[WT Pairs n = 11, *Scn2a*$^{\Delta 1a/+}$ Pairs n = 12]

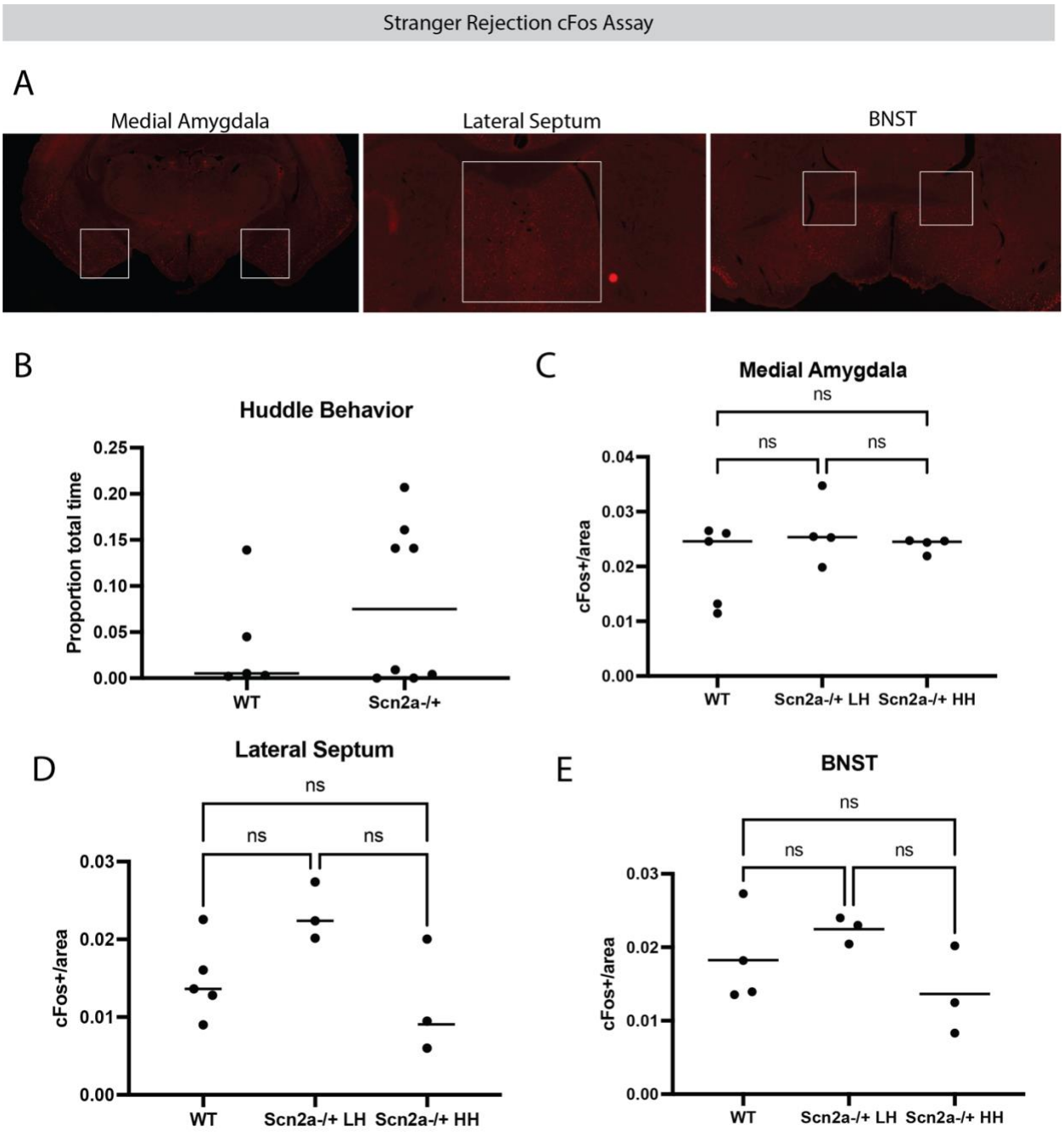

Figure 8: Results from the Stranger Rejection cFos Assay.

A. Representative images of the cFos expression in the MeA (left), LS (middle), and BNST (right) of a male vole.
B. Proportion of time spent engaging in side-by-side huddle behavior with the novel female by male *Scn2a*$^{\Delta 1a/+}$ males (n = 8) and WT sibling males (n = 5).
C. Quantification of cFos+ cells normalized by ROI area in the MeA per group.
D. Quantification of cFos+ cells normalized by ROI area in the LS per group.
E. Quantification of cFos+ cells normalized by ROI area in the BNST per group.

[For all plots: Mann Whitney tests, ns not significant.]

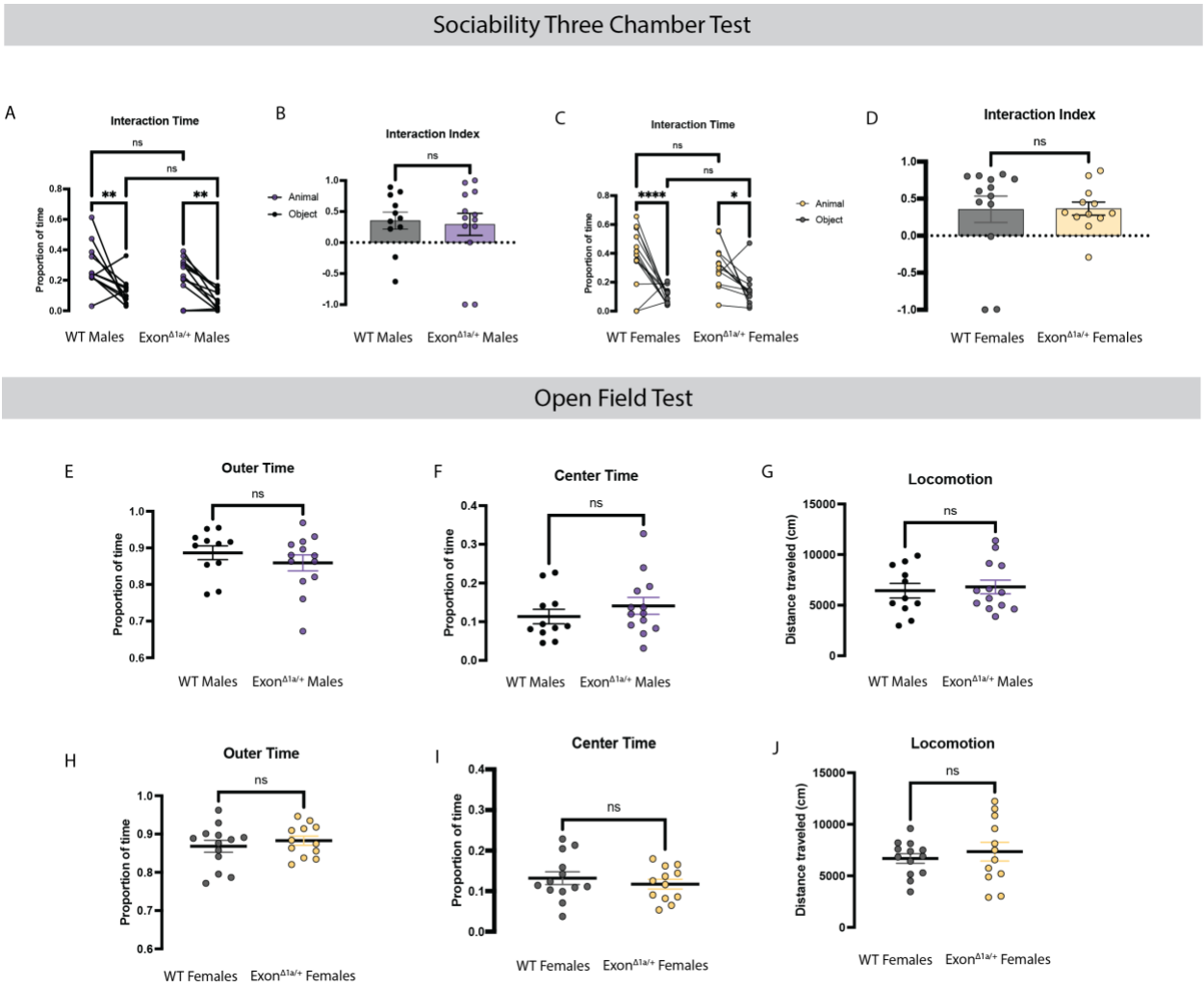

Figure 9: *Scn2a* heterozygosity does not affect anxiety-related behaviors in male or female voles.

A. Time spent by *Scn2a*$^{\Delta 1a/+}$ males and WT sibling males interacting with the novel animal zone or the object zone in the TCT.
B. Preference index indicating that both *Scn2a*$^{\Delta 1a/+}$ males and WT sibling males preferred to spend time with interacting with novel animal zone over the object zone.
C. Time spent by *Scn2a*$^{\Delta 1a/+}$ females and WT sibling females interacting with the novel animal zone or the object zone in the TCT.
D. Preference index indicating that both *Scn2a*$^{\Delta 1a/+}$ females and WT sibling females preferred to spend time with interacting with novel animal zone over the object zone.
E. There is no difference between *Scn2a*$^{\Delta 1a/+}$ males and WT sibling males in proportion of time spent near the edges of the OFT.
F. There is no difference between *Scn2a*$^{\Delta 1a/+}$ males and WT sibling males in proportion of time spent near the edges of the OFT.
G. There is no difference between *Scn2a*$^{\Delta 1a/+}$ males and WT sibling males in proportion of time spent in the center of the chamber of the OFT.

(Figure caption continued on the next page.)

(Figure caption continued from the previous page.)

H. There is no difference between *Scn2a*$^{\Delta 1a/+}$ males and WT sibling males in locomotion in the OFT.
I. There is no difference between *Scn2a*$^{\Delta 1a/+}$ females and WT sibling females in proportion of time spent near the edges of the OFT.
J. There is no difference between *Scn2a*$^{\Delta 1a/+}$ females and WT sibling females in proportion of time spent in the center of the chamber of the OFT.
K. There is no difference between *Scn2a*$^{\Delta 1a/+}$ females and WT sibling females in locomotion in the OFT.

[n = 12 for all groups]

Chapter 2: In situ validation of bulk RNA sequencing results

Introduction

Vasopressin (*AVP*) and Oxytocin (*OXT*) neuropeptide signaling in the brain of prairie voles was thought to be essential for pair bond formation[27–31]. Most of these studies used pharmacological approaches to perturb signaling in the brain of an adult animal. Previous work in the Manoli lab sought to understand the developmental role of Oxytocin receptor (*Oxtr*) signaling in prairie vole pair bonding behavior by generating whole-animal knockouts for *Oxtr*[16,17]. Multiple techniques were then used to characterize these knockout animals, ranging from molecular and cellular to behavioral approaches. For molecular characterization, members of the Manoli lab collected bulk RNA sequencing (RNAseq) data from the vole nucleus accumbens (NAc) of male and female WT and *Oxtr*$^{-/-}$ voles in different stages of pair-bonding. This experiment resulted in several significantly differentially expressed (DEX) genes between *Oxtr*$^{-/-}$ and WT voles, regardless of bonding status. We then wanted to validate the expression changes found in a subset of these DEX genes. Additionally, we were interested in investigating expression changes in these genes in other brain regions and determining if we could specifically uncover evidence of coordinated regulation across the brain.

To validate the sequencing results and to test the coordinated regulation hypothesis, I generated RNA in situ hybridization (ISH) probes to several of the most differentially expressed genes from the bulk sequencing results. I then used these probes to stain and compare the expression of the genes in the NAc of adult prairie vole brains, male and female, pre- and post-cohabitation to validate the expression differences found in the RNA sequencing results. I was able to validate the bulk RNAseq results of a subset of the DEX genes tested in the NAc. I also found evidence of coordinated regulation by Oxtr signaling of two of these genes, Calcr and Dlk1, such that there were expression differences in these genes between *Oxtr*$^{-/-}$ females and WT females in the paraventricular nucleus of the hypothalamus (PVN) and the lateral septum (LS) that mirrored the expression differences found in the NAc.

Results

Generation of prairie vole specific ISH probes

To start the bulk RNAseq validation process, I first took the list of the top 25 DEX genes by p-value and log(foldchange) and designed 1-2 pairs of primers for each gene that would produce a PCR product of 400-1000 base pairs and spanned at least 2 exons to build an ISH RNA probe template. I then used vole brain cDNA as template DNA with the primers for an amplifying PCR program, the success of which was determined by gel electrophoresis. If the gel showed a single band PCR product that corresponded to the predicted size, I then used the ThermoFisher Blunt TOPO vector to transform the PCR product into the TOPO backbone and cloned into bacterial colonies. After processing and preparing the colonies, the plasmids were sent for Sanger sequencing, from which the results were aligned to the published, annotated prairie vole genome using NCBI BLAST to confirm whether the PCR product was a match of the gene of interest. For the probes that were confirmed to be the correct sequence, I moved forward with our protocol for in vitro transcription to turn the plasmid DNA into a single-stranded RNA probes and then tested the binding efficiency of the probes on perfused vole brain tissue mounted on microscope slides using our ISH protocol.

I tested each of the completed RNA probes (18 total) on male and female samples for wildtype and *Oxtr*$^{-/-}$ mutants, pre- or post-bonding. I screened each of the probes on one sample microscope slide from each experimental group depending on the significant result from the bulk RNA sequencing analysis (Table 1). The purpose of this was to test 1) if the probes bound to RNA in the tissue such that we saw visual signal from each probe, 2) if we saw signal from the probe in the NAc, validating the reads in the sequencing results, and 3) if there were noticeable visual differences in the experimental groups based on the DEX results (i.e., post-cohabitation *Oxtr*$^{-/-}$ female vs wildtype female). To assess the third stated goal, I gave the samples to three other lab members and had them blindly judge if they saw probe signal in the NAc and to rate the strength

of the signal on a scale from 0-3. If there was a consensus on a visible difference between the two slides, then we would move forward with that gene.

Of the18 tested genes, I found 2 genes that met all 3 criteria: Calcr and Dlk1. Both genes were found to be differentially expressed between *Oxtr*$^{-/-}$ females and WT females in the bulk RNAseq results such that the expression of the genes was higher in WT females (Fig. 10A). These results were validated by the ISH staining (Fig. 10B,C). I also found significant decreases in Calcr and Dlk1 RNA expression in the PVN and the LS of *Oxtr*$^{-/-}$ females compared to WT females (Fig. 10B,C). These results suggest that there is coordinated regulation of these genes by Oxtr signaling in multiple brain regions such that loss of Oxtr signaling affects RNA expression of genes in a parallel fashion.

Discussion

Here I described the validation process of bulk RNAseq results using ISH staining with probes made in house specifically conjugated to a selection of the DEX genes. I was able to validate the DEX results using this method for two of the genes that showed significant decrease in RNA transcripts in the NAc of *Oxtr*$^{-/-}$ females compared to WT females: Calcr and Dlk1. Furthermore, each of these genes showed evidence of Oxtr signaling regulation in other brain regions such that there was decreased expression of both transcripts in the PVN and the LS of *Oxtr*$^{-/-}$ females compared to WT females. These data support our hypothesis that there might be coordinated regulation of genes in multiple brain regions by Oxtr signaling that would result in similar changes in gene expression with the loss of signaling.

Materials & Methods

Animals: Subjects were laboratory-bred prairie voles (*Microtus ochrogaster*) which originated through systematic outbreeding of a wild stock captured near Champaign, Illinois. Sexually naïve male and female animals were group weaned at 21 ± 5 days separated to group housing with

same-sex siblings and age-matched same-sex non-siblings. Voles were maintained under a 14:10 h light-dark cycle in clear plastic cages 673 (45 × 25 × 15 cm) with bedding, nesting material (nestlet), and a PVC hiding tube. Rooms were maintained at approximately 20°C, and food and water were available *ad libitum*.

In situ hybridization: ISH was performed using RNA probes prepared as described previously, to detect expression of *Calcr* and *Dlk1* mRNA in the adult vole brain. We prepared RNA sense and anti-sense probes corresponding to 706bp (CalcR) and 796bp (Dlk1) for genes of interest identified in the WT vs *Oxtr*$^{-/-}$ DEX list from our RNAseq data. For ISH on adult animals, 7-to 9-week-old WT and *Oxtr*$^{1-/-}$ voles of both sexes were either group housed with same sex conspecifics or paired for 4 days with a WT animal of the opposite sex following the timed mating protocol described above. The brains were processed as described for IHC in Chapter 1, then embedded in OCT and sectioned at 50µm, mounted immediately after sectioning onto SuperFrost Plus glass microscope slides and stored at -80°C until ISH staining. Slides were fixed in 4% PFA for 20 minutes, rinsed in PBS, treated with proteinase K (10µg/mL, Roche) for 20 minutes, rinsed in PBS, and fixed again in 4% PFA for 5 minutes at room temperature. Slides were acylated for 10 mins then rinsed in 1% Triton100X in PBS followed by PBS. The slides were equilibrated in warm hybridization solution for 1-2 hours at 65°C and subsequently incubated with a temporary paraffin cover for 14 - 18 hours at 65°C in fresh hybridization buffer containing RNA probe. After incubation, the slides were dipped in 5X SSC warmed to 72°C to remove the parafilm coverslips and then washed in 0.2X SSC warmed to 72°C. The slides were blocked with 10% heat inactivated sheep serum (HISS) solution then stained for 12 - 18 hours at 4°C in buffer containing 10% HISS and alkaline phosphatase-conjugated sheep anti- digoxigenin antibody (1:2000, Roche). After extensive washing, the slides were incubated for ~72 hours at 37°C in staining solution containing nitro blue tetrazolium and 5- bromo-4-chloro-3-indolyl-phosphate (Roche). The slides were finally washed, fixed in 4% PFA, and cover-slipped. Slides were imaged using a

Keyence fluorescence microscope and the z-stacks were quantified (cell count and area) in ImageJ. For signal quantitation, positive puncta were counted in every third coronal section encompassing the entire anterior to posterior gene expression domain. Cell counts were normalized by total area for a gene expression domain in each section. Positive signal was quantified by calculating total area of signal multiplied by the average intensity of signal (total area x mean pixel intensity) in gene expression domains of a section; every third section was quantified and added. Comparisons of cell counts were made in age and sex matched samples.

Tables

Table 2: DEX genes from the bulk RNAseq results that resulted in successful probes. Bolded text are the genes that showed coordinated expression in other regions. P_{adj} = adjusted p-value.

GeneID	log2FoldChange	p_{adj}	GeneSymbol	comparison
ENSMOCG00000020811	**-1.11831777**	**9.57E-09**	***Calcr***	***Oxtr*$^{-/-}$ vs. WT**
ENSMOCG00000010948	-0.808312524	4.04E-15	*Apod*	*Oxtr*$^{-/-}$ vs. WT
ENSMOCG00000019256	-0.518605974	4.38E-19	*Fgfr1*	*Oxtr*$^{-/-}$ vs. WT
ENSMOCG00000004545	**-0.556106975**	**0.017516797**	***Dlk1***	**PostF *Oxtr*$^{-/-}$ vs. WT**
ENSMOCG00000006680	-0.514949561	0.012542871	*Sez6l*	PostF *Oxtr*$^{-/-}$ vs. WT
ENSMOCG00000016403	-0.465005543	0.034595285	*Pcsk1n*	PostF *Oxtr*$^{-/-}$ vs. WT
ENSMOCG00000009710	0.322316252	0.006894577	*Tenm2*	PostF *Oxtr*$^{-/-}$ vs. WT
ENSMOCG00000020489	0.355800784	0.005634246	*Fgf14*	PostF *Oxtr*$^{-/-}$ vs. WT
ENSMOCG00000011761	0.368314064	0.000610501	*Scn2a*	PostF *Oxtr*$^{-/-}$ vs. WT
ENSMOCG00000022680	0.397187891	0.027613086	*Pdyn*	PostF *Oxtr*$^{-/-}$ vs. WT
ENSMOCG00000010035	0.466548257	4.20E-05	*Ppp1r9a*	PostF *Oxtr*$^{-/-}$ vs. WT
ENSMOCG00000020214	0.488383533	0.003012536	*Epha7*	PostF *Oxtr*$^{-/-}$ vs. WT
ENSMOCG00000005546	0.502742617	0.000425778	*Dgkb*	PostF *Oxtr*$^{-/-}$ vs. WT
ENSMOCG00000007289	0.502899458	8.04E-07	*Taok1*	PostF *Oxtr*$^{-/-}$ vs. WT
ENSMOCG00000001527	0.544276342	9.87E-05	*Atxn1*	PostF *Oxtr*$^{-/-}$ vs. WT
ENSMOCG00000016596	0.711022721	0.000396577	*Pde10a*	PostF *Oxtr*$^{-/-}$ vs. WT
ENSMOCG00000019383	0.964961551	1.87E-08	*Thsd7a*	PostF *Oxtr*$^{-/-}$ vs. WT
ENSMOCG00000016578	1.243232081	0.003518502	*Sstr2*	PostF *Oxtr*$^{-/-}$ vs. WT

Figures

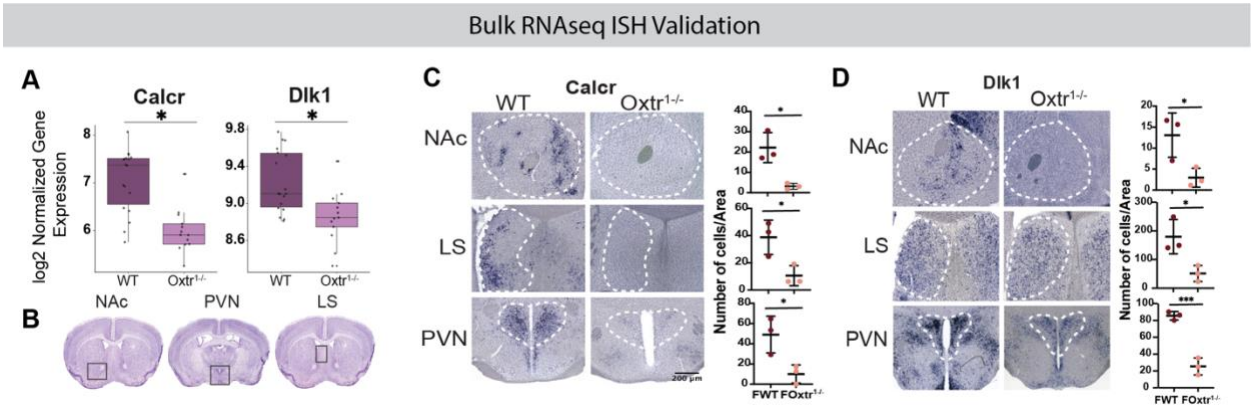

Figure 10: Results of Calcr and Dlk1 ISH validation

A. Quanitification of Calcr and Dlk1 expression in the NAc of WT females (dark purple,n=3) and *Oxtr*$^{1-/-}$ females (light purple, n=3) showing a significant decrease in expression in the *Oxtr*$^{1-/-}$ females.
B. Representative images of the regions of interest for quanitification: NAc (left), PVN (middle), and LS (right).
C. Representative images of Calcr mRNA expression in the NAc, LS, and PVN of WT females and *Oxtr*$^{1-/-}$ females. Quantification demonstrating a significant decrease in expression in all 3 brain regions in *Oxtr*$^{1-/-}$ females compared to WT females.
D. Representative images of Dlk1 mRNA expression in the NAc, LS, and PVN of WT females and *Oxtr*$^{1-/-}$ females. Quantification demonstrating a significant decrease in expression in all 3 brain regions in *Oxtr*$^{1-/-}$ females compared to WT females.

Chapter 3: CRISPR-mediated Mutagenesis & Transgenesis

Introduction

Prairie voles (*Microtus ochrogaster*) do well in a lab environment, have conserved genetics and neural circuitry, display a robust repertoire of social behavior not found in many other lab species [15,32–35]. Prairie voles are also maintained as an outbred species and therefore are a strong model for translational studies because the variety in genetic background leads to variability in behavioral and neural responses[36,37]. Futhermore, the prairie vole genome has been mapped and annotated, which gives us access to their genetics in a way that allows us to potentially manipulate the genome of an animal[38,39]. However, relative to more traditional model species, there are very few genetic tools in the prairie vole, limiting our ability to understand the impact of developmental genetic mutations on social behavior and underlying neural circuitry. Moreover, there are no transgenic models that would allow us to manipulate gene expression in the prairie vole genome beyond using spatially-constrained viral techniques.

To address this need in the field, the Manoli Lab has developed a protocol to manipulate the prairie vole genome. We have routinely and reliably used the CRISPR system with both microinjections and electroporation and house made or Dharmacon RNA guides to make prairie vole lines mutant for several genes of interest[40–43]. This has allowed us to explore the developmental impacts of loss of function mutations in these genes on social behaviors. We have found social behavior differences in developmental knockout animals of both heterozygous (*Scn2a* and *Shank3*) and homozygous mutations (*Oxtr*), establishing the prairie vole as a powerful model for studying social circuitry and modeling human disorders characterized by social differences. Given the success of our mutagenesis approach, we next wanted to adapt our protocol to generate Cre-recombinase knock-in and other transgenic prairie voles.

Results

CRISPR-mediated transgenesis

Our predominant strategy, based on what has been successful in other model organisms, was to use the CRISPR/Cas9 system and single-stranded DNA (ssDNA) as donor DNA to be integrated into the genome[43]. We have also attempted strategies using plasmids and melted double-stranded DNA (dsDNA), or a combination of donor DNA types. We so far have attempted to knock-in Cre-recombinase under the *Oxtr* promotor in 2 different locations – one that would integrate in the coding region of the gene and result in a non-functional copy of *Oxtr* and one that only disrupts the stop codon at the end of the coding sequencing, leaving the coding sequence intact and able to produce a functional copy of the gene. We have also generated template DNA to create a vole FosTRAP model[44]. The specific sequences of donor DNA include varying lengths of overlapping genomic sequence on either side of the Cre-recombinase or Cre-ER that we intend to knock into the chosen locus (Fig. 11A-C).

To produce the donor ssDNA, I start with a highly concentrated dsDNA plasmid containing our knock-in sequence flanked by prairie vole genomic DNA sequence for our locus of interest as the template. I designed primers or that would produce a PCR product with genomic sequence arms 90-600 base pairs in length. As we continue optimizing this process, the flanking arm length is one of the aspects we are modifying to find the most efficient arm length for integration. Longer arms (~400-600+ base pairs) provide better specificity of homologous recombination in the targeted locus, however, I it is difficult to confirm locus-specific integration with PCR and Sanger sequencing alone because the resulting PCR products from the screen needed to be extremely large to capture sequence outside of the arm sequence. Shorter arms (~90-200 base pairs) address the issue of screening PCR feasibility after generating G0 animals, but we have not found more success with proper insertion of our donor DNA.

We have attempted both electroporation and microinjections of our previously successful CRISPR/Cas9 reagent mix with the addition of our donor DNA and guides of choice. We

attempted a range of amounts of DNA, from 5ugs to 20ugs, and have found evidence that much more DNA is required for integration than has been published to be successful in other species[43]. After the CRISPR reagents were applied to the single-cell embryos using either method, the embryos were incubated and grown to the blastocyst stage, and the healthy blastocysts were implanted into a pseudopregnant female who was paired with a vasectomized male. The pups born from these surgeries were considered the G0 generation for each round of implantation. We also assume that the G0s produced from the implanted female are chimeras, and therefore opt to breed each one with a WT partner to produce F1 litters, which we expect to be heterozygous for any mutations we introduced in the G0s' genomes.

PCR validation of donor DNA integration

To identify a successful knockin, I developed several genotyping schemes for each intended transgenic model for screening. Given that each F1 can at most carry one allele from the G0, these were the animals screened for successful integration. This would also be informative as to whether the mutations were transmissible given that they would have already been passed down from the G0 to the F1 generation. I designed primers targeted to genomic DNA inside and outside the donor arm region, and primers that were specific to the sequence of exogenous DNA (i.e., Cre-recombinase), and attempted to run a PCR using multiple combinations of each of these primer types. If I was able to isolate a clean single band from a PCR of the predicted size, then I would attempt to confirm the band corresponded to successful integration of our donor DNA. After several attempts, I was not able to reliably or consistently run a PCR that confirmed integration. However, despite not developing a robust PCR scheme that could be used to routinely screen and identify progeny with successful integration, I occasionally found evidence of Cre-recombinase sequence in DNA samples from animals and would continue outcrossing these animals in attempt to propagate the transgenic lines.

P0 pup injection protocol development and functional validation

In parallel to developing genotyping schemes, I attempted to validate the functionality of potential Cre-recombinase integration by injecting animals with a Cre-dependent fluorescent virus. Rather than doing a full stereotaxic surgery on adults, I instead decided to adapt a P0 untargeted injection protocol for neonatal prairie voles[45,46]. I first tested the approach with constitutive fluorescent viruses in WT animals to gauge the range of expression I could achieve across the brain (Fig 12A). This method proved to be relatively quick compared to an adult stereotaxic surgery and extremely effective for screening viral expression, as I was able to achieve cortical to whole brain-wide expression, depending on the serotype, at P14 and P21.

After validating the approach, I then began injecting neonates born to F1 crosses from our suspected transgenic lines. Using the same protocol, I injected all animals in a litter with the same fluorescently tagged Cre-dependent virus. I gave each animal in a litter the same virus because there was no way to identify individuals when I collected brain tissue for processing. Furthermore, given that the virus can only express its fluorescent tag if there was complete and successful integration of Cre-recombinase somewhere in the genome, so I could then use DNA samples from brains expressing the virus as positive controls for optimization of genotyping protocols. After injecting several litters, I rarely saw more than a handful of cells expressing the fluorescent tags (Fig. 12B,C). This could suggest that potentially the viruses used were leaky and the Cre-dependent fluorescent tag was expressing even in the absence of Cre-recombinase. It could also indicate that Cre-recombinase was randomly integrated into the genome, though not in our intended locus, and therefore allowing recombinant expression of a Cre-dependent fluorescent tag at low levels.

I attempted similar functional validation of FosTRAP F1s, but using adults that would display behaviors that would induce cFos expression. We also struggled to confirm Cre-ER integration under the vole *cFos* promotor using PCR and sequencing methods, so functional validation could potentially provide positive control samples for development and optimization of

this PCR scheme. To achieve this, I injected a Cre-dependent virus into the LS of adult prairie voles, male or female, born to G0 and F1 pairs from FosTRAP transgenic lines. I chose the LS because it is a large nucleus and easy to target with this type of injection, and has shown evidence of neural activation in prairie voles with a variety of social stimuli. The animals were then given 2 weeks to recover from surgery before then being exposed to an opposite-sex conspecific after a tamoxifen injection to induce Cre-ER function in animals carrying the FosTRAP construct (animals negative for the mutation would theoretically serve as controls). If the construct was functional in the animals, the then activated Cre-ER would recombine the viral construct and cells activated by the stimulus animal would express mCherry under the cFos promotor. Animals were then co-housed with the stimulus animal for 2 weeks before going through a Partner Reunification Assay as described in Chapter 1 methods. After the behavioral interaction period, the animals from the FosTRAP transgenic pairs were perfused and brain tissue was collected for processing. Brain sections from these animals were stained for cFos as well as the fluorescent protein to amplify the virus signal. Each animal showed robust cFos expression induced by the Partner Reunification Assay, but only a subset of animals showed evidence of “trapped” virus expression induced by the introduction of the soon-to-be cohabitated partner in the LS (Fig. 12D,E). This suggests that our construct was potentially integrated into the G0 genome, however further work is still needed to validate the success of the procedure with a PCR scheme that can be used for genotyping purposes.

Discussion

Here, I described my contribution to the optimization of our protocol for generating transgenic prairie vole models. We have attempted several different conditions using various types of donor DNA to knockin Cre-recombinase or Cre-ER into our locus of interest. I have found some evidence of functional integration of both knockin constructs by expression of Cre-dependent fluorescent proteins in juvenile and adult brain sections, with and without IHC signal

amplification. However, we have not been able to confirm through PCR and Sanger sequencing that our donor DNA sequence was successfully integrated into the target locus. This suggests that we were potentially succeeded at random integration of our complete construct somewhere in the genome of G0s such that the Cre-recombinase portion is functional. This is further supported by the fact that we often saw sparse cell labeling in some of the brain tissue collected from injected animals, but not at the levels we would expect if the Cre-recombinase was transcribed under the *Oxtr* promotor.

Further optimization is needed for our electroporation or injection conditions so that we can achieve successful integration. Given that we have such high success rates with knocking out genes, we are confident that we can eventually find the optimal conditions for knocking in DNA. Optimization will include screening old and new sgRNAs for cutting efficiency when the embryos reach the blastocyst stage, and modifying the concentrations of sgRNAs and donor DNA injected to improve the hit rate of embryos with mutations. We can also continue to manipulate the donor DNA arm length to find the best size for specific integration. Lastly, to increase the efficiency of validating the integration of our donor DNA, we could send our DNA sample for whole-genome sequencing rather than relying on PCR protocols, which are limited by the placement and specificity of primers. This way we can know definitively if we have successfully knocked in our transgenes and where the transgene is located.

Materials & Methods

Animals: Subjects were laboratory-bred prairie voles (*Microtus ochrogaster*) which originated through systematic outbreeding of a wild stock captured near Champaign, Illinois. Sexually naïve male and female animals were group weaned at 21 ± 5 days separated to group housing with same-sex siblings and age-matched same-sex non-siblings. Voles were maintained under a 14:10 h light-dark cycle in clear plastic cages 673 (45 × 25 × 15 cm) with bedding, nesting material

(nestlet), and a PVC hiding tube. Rooms were maintained at approximately 20°C, and food and water were available *ad libitum*.

CRISPR-mediated transgenesis: Embryo harvesting and manipulation occurred as previously described[17]. Briefly, adult male and female prairie voles were paired and put through a timed mating protocol to induce estrus and yield time-locked fertilization. Embryos were then harvested from the females and injected or electroporated with donor DNA, Cas9 mRNA, Cas9 protein, and short guide RNAs (sgRNAs) to the targeted locus. Embryos were then cultured to the blastocyst stage before being implanted in a pseudopregnant female for gestation.

Table 3: sgRNA sequences used for transgene integration.

Gene Locus	sgRNA Sequence	Source
Oxtr	GCCACCACCAGGTCAGCGATGCTC	In house
Oxtr	CAGCTGCTGTGGGACATCACCTTC	In house
Oxtr end	TCTTCAGCATGAGCCACCTGTC	Dharmacon
Oxtr end	GCAGGCGCGGTGGGCCAGACAGG	Dharmacon
cFos	CACTACTCGCCCTGTGAGCGGTC	Dharmacon
cFos	CCTCCCCTTCCCTGACCGCTCAC	Dharmacon

Neonate injections: All P0 pups from a litter are first removed from the parental cage no less than three hours after birth. Often the pups would be nursing and attached to the mother, but can easily be detached by gently pulling on the pup. Each pup was removed at the same time and placed on a paper towel-wrapped metal surface placed on a bed of ice for cryoanesthesia. The pups laid on the cold metal for a minimum of 5 minutes until the breathing slowed and the movements were significantly reduced. When the pups were sufficiently cryoanesthetized, 1-2ul of virus (list of viruses below) was passively taken up by a pulled glass capillary needle. The filled needle is then attached to a tubing system that fits a pipette tip on the other end so that a pipette can be attached, allowing for control of the virus release in the brain. Carefully, without breaking the needle tip, puncture the skin and skull of the pup, aiming for the lateral ventricle on either side of the midline.

Slowly plunge the pipette to control speed of virus injection. When the full virus volume is completely injected into the brain, carefully remove the capillary needle dispose in a sharps container. Use a fresh needle for each pup to avoid clogging of the needles. After each pup in a litter was injected, they were all placed onto heating pad to slowly warm up. Once the pups are moving and breathing normally, they are returned to the nest of the parental cage.

Table 4: List of viruses tested in neonates.

Viruses tested at P0	Source
AAV8-CAG-tdTomato	Addgene
AAV8-CBA-GFP	Addgene
AAV9-CBA-GFP	Addgene
AAV1-CBA-GFP	Addgene
AAV5-CBA-GFP	Addgene
PHP.eB-CAG-GFP	Addgene
pAAV-hSyn-DIO-mCherry (AAV8)	Addgene
pAAV-EF1a-Nuc-flox(mCherry)-EFGP) (AAV9)	Addgene
PHP.eB-CAG-FLEX-tdTomato	Addgene
PHP.eB-CAG-EGFP	Addgene

Stereotaxic Injections: Adult voles from FosTRAP breeding pairs were anesthetized with isoflurane and administered bupivacaine subcutaneously at the incision site. Using a stereotaxic frame (Kopf Instruments, Tujunga, CA), a craniotomy was made +0.8 mm anterior and +0.35 mm lateral relative to bregma, and a 33-gauge cannula was lowered to -4.0 mm relative to bregma. I injected 1:1 virus mix of PHP.eB-CAG-FLEX-tdTomato and PHP.eB-CAG-EGFP. I infused 1 µL of virus at a rate of 0.1 µL/min via an automated injection system (Genie Touch, Kent Scientific Corporation, Torrington, CT). The cannula was left in place for ten minutes to allow for viral diffusion, then was slowly removed to minimize viral infection along the needle tract. Following viral injection, the wound was closed with CellPoint Scientific Reflex 7mm wound clips and animals received postoperative buprenorphine and recovered for two weeks prior to testing.

FosTRAP Behavior experiments: Two weeks after the viral injection surgery, voles potentially containing the FosTRAP construct were injected with 10mg/mL 4-OHT dissolved in corn oil (4-Hydrotamoxifen, Sigma, Cat #H6278 and Corn oil, Sigma, Cat #C8267) immediately introduced to an age-matched, opposite-sex conspecific that will become the subject vole's cohabitated partner. The pairs were housed normally for 2 weeks and then went through a modified Partner Reunification assay where the subject animal was separated from its partner for a 1-hour isolation period in its home cage before the partner was reintroduced to the home cage for 90 minutes. The subject animal was then perfused for brain dissection and processing.

Histology: Animals were perfused for fixation and brains were dissected as described in Chapters 1 and 2. For the P0 virus screens, perfusions for tissue collection happened at P14 or P21, the tissue was post-fixed overnight and cryoprotected in 30% sucrose before sectioning. I collected 50um sections and mounted the entire brain on microscope slides. Whole-slide images were taken on the Keyence-BZ fluorescent microscope for surveying expression. For FosTRAP behavior experiments, perfusions happened immediately after the Partner Reunification assay, the tissue was processed, sectioned, and stained using the IHC protocol described above with primary antibodies (cFos Monoclonal Antibody, Synaptic Systems, Rat Monoclonal, Cat #226017, 1:5000 and GFP Polyclonal Antibody, Abcam, Chicken Polyclonal Cat #ab13970, 1:1200) and secondary antibodies (Cy™3 AffiniPure Donkey Anti-Rat IgG, Jackson ImmunoResearch Laboratory, Cat #711-165-150, 1:500 and Alexa Fluor® 488-conjugated AffiniPure Donkey Anti-Chicken IgY††(IgG), Jackson ImmunoResearch Laboratory, Cat #703-545-155, 1:500). Mounted sections were imaged on the Keyence-BZ microscope for surveying expression.

Figures

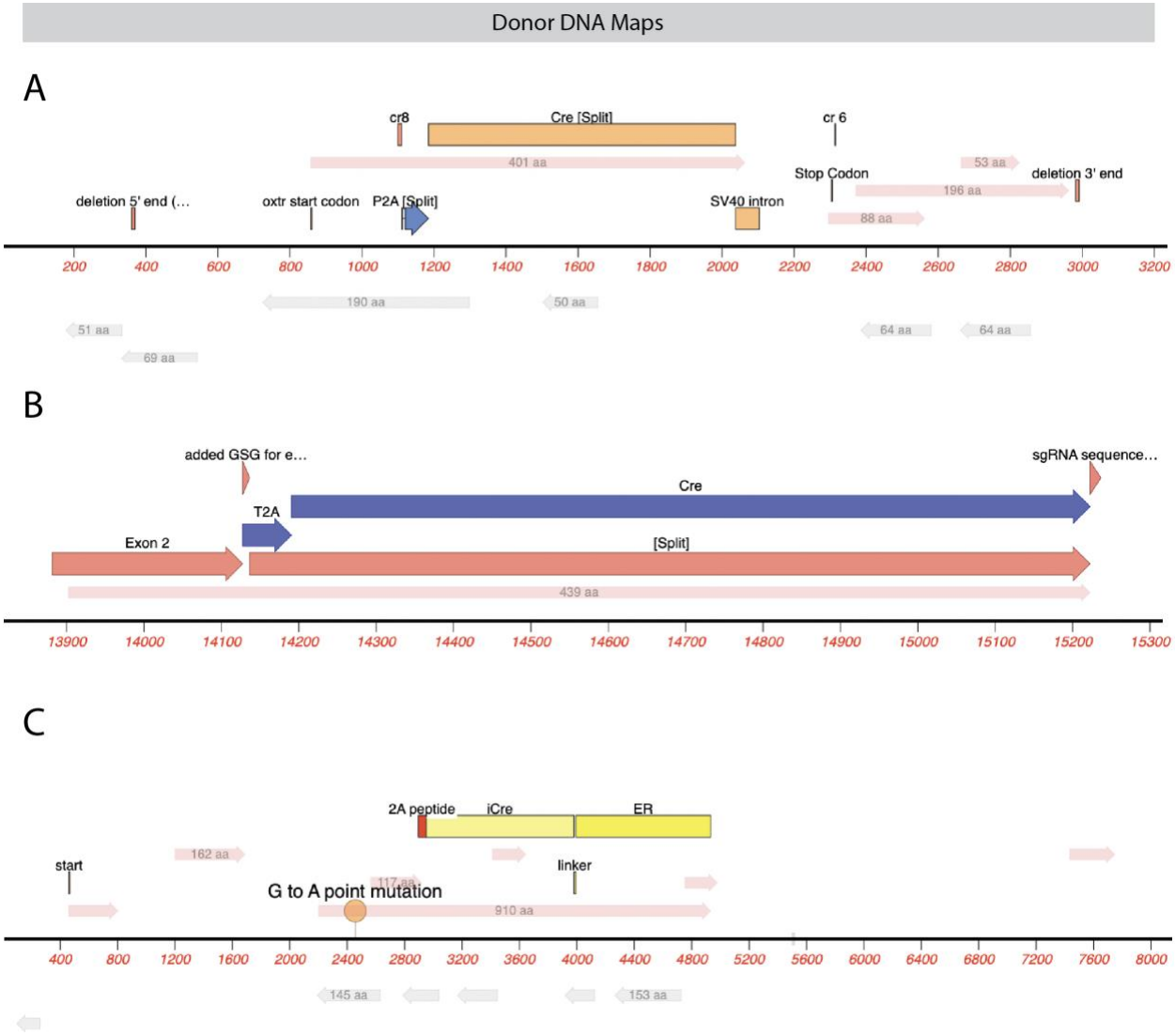

Figure 11: Maps of donor DNA sequences integrated into loci of interest.

A. Map of the knockin/knockout *Oxtr*-cre donor DNA sequence that would result in a null copy of *Oxtr*.
B. Map of the *Oxtr*-cre donor DNA sequence that would inset at the end of *Oxtr* exon 2.
C. Map of the vole FosTRAP DNA.

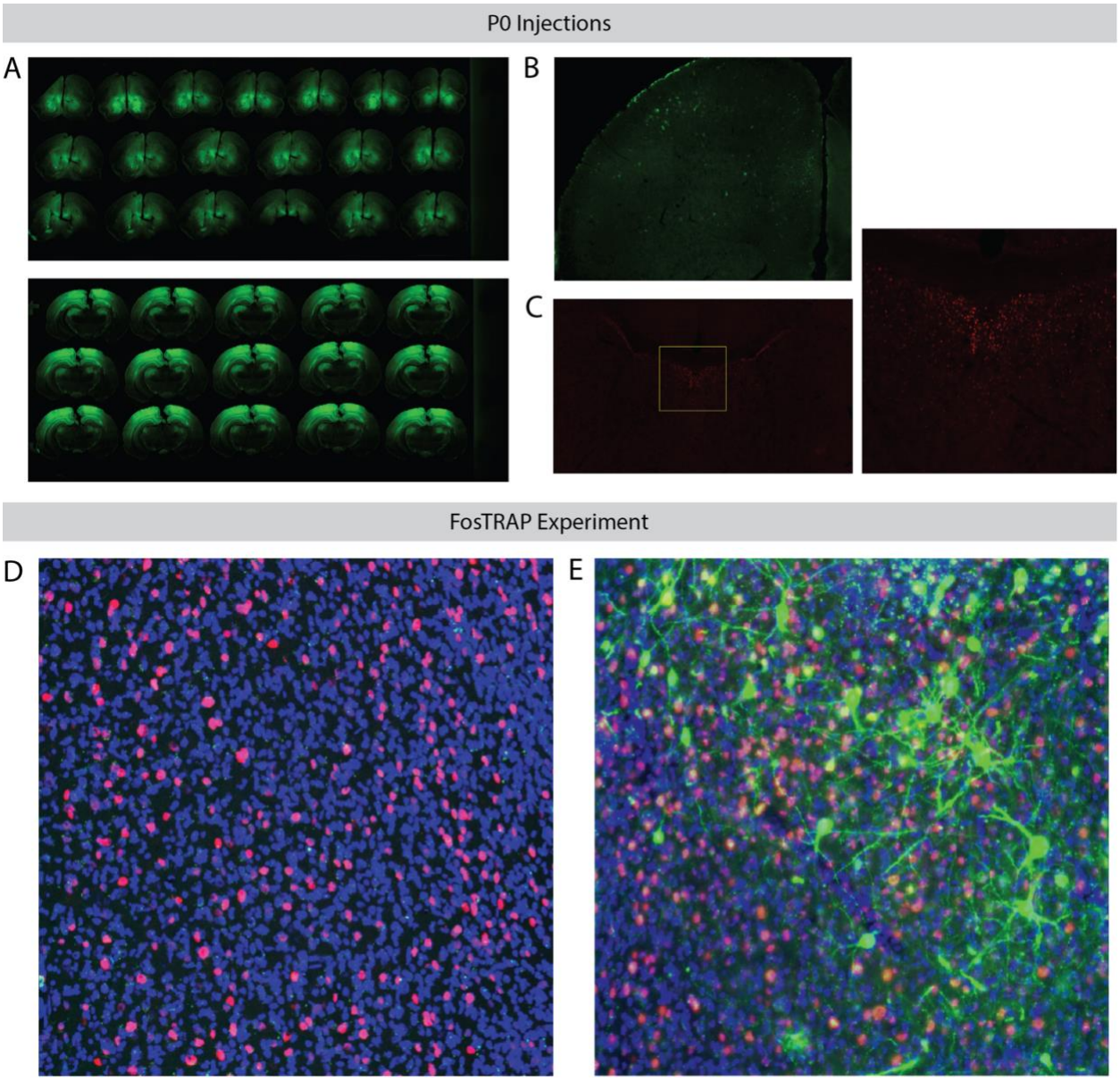

Figure 12: Cre-dependent expression of fluorescent reported viruses.

A. Representative images of whole brain sections from a P14 vole that was injected with PHP.eB-CAG-GFP at P0. GFP was found in the most anterior sections (top) and most posterior sections (bottom) collected from this brain.
B. Representative image showing sparse Cre-dependent GFP fluorescent labelling in neurons in the anterior cortex of a P14 animal injected at P0.
C. Representative image showing mCherry-labeled cells in the LS of a P14 vole injected with a Cre-dependent fluorescent virus at P0.
D. cFos antibody expression (red) but no GFP in the LS of a FosTRAP animal injected with a GFP Cre-dependent virus before tamoxifen injection and a behavior assay.

(Figure caption continued on the next page.)

(Figure caption continued from the previous page.)

E. cFos antibody expression (red) and GFP virus expression (green) from a TRAPed neurons in the LS of a FosTRAP animal injected with tamoxifen before a behavior assay.

References

1. Carter CS, Getz LL. Monogamy and the prairie vole. *Sci Am*. 1993;268(6):100-106.

2. Insel TR. A neurobiological basis of social attachment. *Am J Psychiatry*. 1997;154(6):726-735.

3. Young LJ, Wang Z. The neurobiology of pair bonding. *Nat Neurosci*. 2004;7(10):1048-1054. doi:10.1038/nn1327

4. Neurodevelopmental Disorders. In: *Diagnostic and Statistical Manual of Mental Disorders*. DSM Library. American Psychiatric Association; 2013. doi:10.1176/appi.books.9780890425596.dsm01

5. Fu JM, Satterstrom FK, Peng M, et al. Rare coding variation provides insight into the genetic architecture and phenotypic context of autism. *Nat Genet*. 2022;54(9):1320-1331. doi:10.1038/s41588-022-01104-0

6. Satterstrom FK, Kosmicki JA, Wang J, et al. Large-Scale Exome Sequencing Study Implicates Both Developmental and Functional Changes in the Neurobiology of Autism. *Cell*. 2020;180(3):568-584.e23. doi:10.1016/j.cell.2019.12.036

7. Sanders SJ, Murtha MT, Gupta AR, et al. De novo mutations revealed by whole-exome sequencing are strongly associated with autism. *Nature*. 2012;485(7397):237-241. doi:10.1038/nature10945

8. Ben-Shalom R, Keeshen CM, Berrios KN, An JY, Sanders SJ, Bender KJ. Opposing Effects on Na(V)1.2 Function Underlie Differences Between SCN2A Variants Observed in Individuals With Autism Spectrum Disorder or Infantile Seizures. *Biol Psychiatry*. 2017;82(3):224-232. doi:10.1016/j.biopsych.2017.01.009

9. Spratt PWE, Ben-Shalom R, Keeshen CM, et al. The Autism-Associated Gene Scn2a Contributes to Dendritic Excitability and Synaptic Function in the Prefrontal Cortex. *Neuron*. 2019;103(4):673-685.e5. doi:10.1016/j.neuron.2019.05.037

10. Léna I, Mantegazza M. NaV1.2 haploinsufficiency in Scn2a knock-out mice causes an autistic-like phenotype attenuated with age. *Sci Rep*. 2019;9(1):12886. doi:10.1038/s41598-019-49392-7

11. Tatsukawa T, Raveau M, Ogiwara I, et al. Scn2a haploinsufficient mice display a spectrum of phenotypes affecting anxiety, sociability, memory flexibility and ampakine CX516 rescues their hyperactivity. *Mol Autism*. 2019;10:15-15. doi:10.1186/s13229-019-0265-5

12. Kazdoba TM, Leach PT, Yang M, Silverman JL, Solomon M, Crawley JN. Translational Mouse Models of Autism: Advancing Toward Pharmacological Therapeutics. In: Robbins TW, Sahakian BJ, eds. *Translational Neuropsychopharmacology*. Springer International Publishing; 2016:1-52. doi:10.1007/7854_2015_5003

13. Silverman JL, Yang M, Lord C, Crawley JN. Behavioural phenotyping assays for mouse models of autism. *Nat Rev Neurosci*. 2010;11(7):490-502. doi:10.1038/nrn2851

14. Takumi T, Tamada K, Hatanaka F, Nakai N, Bolton PF. Behavioral neuroscience of autism. *Neurosci Biobehav Rev*. 2020;110:60-76. doi:10.1016/j.neubiorev.2019.04.012

15. Carter CS, DeVries AC, Getz LL. Physiological substrates of mammalian monogamy: the prairie vole model. *Neurosci Biobehav Rev*. 1995;19(2):303-314.

16. Sharma R, Berendzen KM, Everitt A, et al. Oxytocin receptor controls promiscuity and development in prairie voles. Published online February 14, 2025. doi:10.7554/eLife.104889.1

17. Berendzen KM, Sharma R, Mandujano MA, et al. Oxytocin receptor is not required for social attachment in prairie voles. *Neuron*. 2023;111(6):787-796.e4. doi:10.1016/j.neuron.2022.12.011

18. Terleph TA. A comparison of prairie vole audible and ultrasonic pup calls and attraction to them by adults of each sex. *Behaviour*. 2011;148(11-13):1275-1294. doi:10.1163/000579511X600727

19. Hurst JL, Payne CE, Nevison CM, et al. Individual recognition in mice mediated by major urinary proteins. *Nature*. 2001;414(6864):631-634. doi:10.1038/414631a

20. Sheng M, Greenberg ME. The regulation and function of c-fos and other immediate early genes in the nervous system. *Neuron*. 1990;4(4):477-485. doi:10.1016/0896-6273(90)90106-P

21. Werling DM, Geschwind DH. Sex differences in autism spectrum disorders. *Curr Opin Neurol*. 2013;26(2):146-153. doi:10.1097/WCO.0b013e32835ee548

22. Werling DM, Parikshak NN, Geschwind DH. Gene expression in human brain implicates sexually dimorphic pathways in autism spectrum disorders. *Nat Commun*. 2016;7:10717-10717. doi:10.1038/ncomms10717

23. Werling DM. The role of sex-differential biology in risk for autism spectrum disorder. *Biol Sex Differ*. 2016;7:58. doi:10.1186/s13293-016-0112-8

24. Clarkson RL, Liptak AT, Gee SM, Sohal VS, Bender KJ. D3 Receptors Regulate Excitability in a Unique Class of Prefrontal Pyramidal Cells. *J Neurosci*. 2017;37(24):5846-5860. doi:10.1523/JNEUROSCI.0310-17.2017

25. Dembrow NC, Chitwood RA, Johnston D. Projection-Specific Neuromodulation of Medial Prefrontal Cortex Neurons. *J Neurosci*. 2010;30(50):16922-16937. doi:10.1523/JNEUROSCI.3644-10.2010

26. Nicholson D, Cohen Y. vak: a neural network framework for researchers studying animal acoustic communication. In: ; 2023:59-67. doi:10.25080/gerudo-f2bc6f59-008

27. Lim MM, Young LJ. Neuropeptidergic regulation of affiliative behavior and social bonding in animals. *Horm Behav*. 2006;50(4):506-517. doi:10.1016/j.yhbeh.2006.06.028

28. Lim MM, Young LJ. Vasopressin-dependent neural circuits underlying pair bond formation in the monogamous prairie vole. *Neuroscience*. 2004;125(1):35-45.

29. Lim MM, Bielsky IF, Young LJ. Neuropeptides and the social brain: potential rodent models of autism. *Int J Dev Neurosci Off J Int Soc Dev Neurosci*. 2005;23(2-3):235-243. doi:10.1016/j.ijdevneu.2004.05.006

30. Bales KL, Kim AJ, Lewis-Reese AD, Sue Carter C. Both oxytocin and vasopressin may influence alloparental behavior in male prairie voles. *Horm Behav*. 2004;45(5):354-361. doi:10.1016/j.yhbeh.2004.01.004

31. Donaldson ZR, Young LJ. Oxytocin, vasopressin, and the neurogenetics of sociality. *Science*. 2008;322(5903):900-904. doi:10.1126/science.1158668

32. McGraw LA, Young LJ. The prairie vole: an emerging model organism for understanding the social brain. *Trends Neurosci*. 2010;33(2):103-109. doi:10.1016/j.tins.2009.11.006

33. Getz LL, Mcguire B, Carter CS. Social behavior, reproduction and demography of the prairie vole, *Microtus ochrogaster*. *Ethol Ecol Evol*. 2003;15(2):105-118. doi:10.1080/08927014.2003.9522676

34. Sun P, Smith a. S, Lei K, Liu Y, Wang Z. Breaking bonds in male prairie vole: Long-term effects on emotional and social behavior, physiology, and neurochemistry. *Behav Brain Res*. 2014;265:22-31. doi:10.1016/j.bbr.2014.02.016

35. Kenkel WM, Gustison ML, Beery AK. A Neuroscientist's Guide to the Vole. *Curr Protoc*. 2021;1(6):e175. doi:10.1002/cpz1.175

36. Ophir AG, Phelps SM, Sorin AB, Wolff JO. Morphological, Genetic, and Behavioral Comparisons of Two Prairie Vole Populations in the Field and Laboratory. *J Mammal*. 2007;88(4):989-999. doi:10.1644/06-MAMM-A-250R.1

37. Vogel AR, Patisaul HB, Arambula SE, Tiezzi F, McGraw LA. Individual Variation in Social Behaviours of Male Lab-reared Prairie voles (Microtus ochrogaster) is Non-heritable and Weakly Associated with V1aR Density. *Sci Rep*. 2018;8(1):1396. doi:10.1038/s41598-018-19737-9

38. McGraw LA, Davis JK, Lowman JJ, et al. Development of genomic resources for the prairie vole (Microtus ochrogaster): construction of a BAC library and vole-mouse comparative cytogenetic map. *BMC Genomics*. 2010;11:70. doi:10.1186/1471-2164-11-70

39. Mcgraw L a, Thomas JW, Young LJ. White paper proposal for sequencing the genome of the prairie vole (Microtus ochrogaster). :1-14.

40. Gupta D, Bhattacharjee O, Mandal D, et al. CRISPR-Cas9 system: A new-fangled dawn in gene editing. *Life Sci*. 2019;232:116636. doi:10.1016/j.lfs.2019.116636

41. Platt RJ, Chen S, Zhou Y, et al. CRISPR-Cas9 Knockin Mice for Genome Editing and Cancer Modeling. *Cell*. 2014;159(2):440-455. doi:10.1016/j.cell.2014.09.014

42. Leal A, Herreno-Pachón A, Benincore-Flórez E, Karunathilaka A, Tomatsu S. Current Strategies for Increasing Knock-In Efficiency in CRISPR/Cas9-Based Approaches. *Int J Mol Sci*. 2024;25(5):2456. doi:10.3390/ijms25052456

43. Yao X, Wang X, Hu X, et al. Homology-mediated end joining-based targeted integration using CRISPR/Cas9. *Cell Res*. 2017;27(6):801-814. doi:10.1038/cr.2017.76

44. Guenthner CJ, Miyamichi K, Yang HH, Heller HC, Luo L. Permanent Genetic Access to Transiently Active Neurons via TRAP: Targeted Recombination in Active Populations. *Neuron*. 2013;78(5):773-784. doi:10.1016/j.neuron.2013.03.025

45. Passini MA, Wolfe JH. Widespread Gene Delivery and Structure-Specific Patterns of Expression in the Brain after Intraventricular Injections of Neonatal Mice with an Adeno-Associated Virus Vector. *J Virol*. 2001;75(24):12382-12392. doi:10.1128/JVI.75.24.12382-12392.2001

46. Chakrabarty P, Rosario A, Cruz P, et al. Capsid Serotype and Timing of Injection Determines AAV Transduction in the Neonatal Mice Brain. Qiu J, ed. *PLoS ONE*. 2013;8(6):e67680. doi:10.1371/journal.pone.0067680

Publishing Agreement

It is the policy of the University to encourage open access and broad distribution of all theses, dissertations, and manuscripts. The Graduate Division will facilitate the distribution of UCSF theses, dissertations, and manuscripts to the UCSF Library for open access and distribution. UCSF will make such theses, dissertations, and manuscripts accessible to the public and will take reasonable steps to preserve these works in perpetuity.

I hereby grant the non-exclusive, perpetual right to The Regents of the University of California to reproduce, publicly display, distribute, preserve, and publish copies of my thesis, dissertation, or manuscript in any form or media, now existing or later derived, including access online for teaching, research, and public service purposes.

DocuSigned by:
Gina Williams
6AAFD49C6CB04D8...
Author Signature

3/19/2025
Date